Asian Journal of Pharmaceutical Sciences 16 (2021) 738–761

Available online at www.sciencedirect.com

ScienceDirect

journal homepage: www.elsevier.com/locate/AJPS

Review

Nanomedicine potentiates mild photothermal therapy for tumor ablation

Zijun Jiang[1], *Tianyi Li*[1], *Hao Cheng, Feng Zhang, Xiaoyu Yang, Shihao Wang, Jianping Zhou, Yang Ding*[*]

Key Laboratory of Drug Quality Control and Pharmacovigilance (Ministry of Education), State Key Laboratory of Natural Medicines, NMPA Key Laboratory for Research and Evaluation of Pharmaceutical Preparations and Excipients, Department of Pharmaceutics, China Pharmaceutical University, Nanjing 210009, China

ARTICLE INFO

Article history:
Received 21 August 2021
Revised 3 October 2021
Accepted 5 October 2021
Available online 15 October 2021

Keywords:
Nanomedicine
Mild temperature PTT
Thermo-resistance
Promote mPTT monotherapy
Synergistic therapy

ABSTRACT

The booming photothermal therapy (PTT) has achieved great progress in non-invasive oncotherapy, and paves a novel way for clinical oncotherapy. Of note, mild temperature PTT (mPTT) of 42–45 °C could avoid treatment bottleneck of the traditional PTT, including nonspecific injury to normal tissues, vasculature and host antitumor immunity. However, cancer cells can resist mPTT via heat shock response and autophagy, thus leading to insufficient mPTT monotherapy to ablate tumor. To overcome the deficient antitumor efficacy caused by thermo-resistance of cancer cells and mono mPTT, synergistic therapies towards cancer cells have been conducted with mPTT. This review summarizes the recent advances in nanomedicine-potentiated mPTT for cancer treatment, including strategies for enhanced single-mode mPTT and mPTT plus synergistic therapies. Moreover, challenges and prospects for clinical translation of nanomedicine-potentiated mPTT are discussed.

1. Introduction

Photothermal therapy (PTT) has emerged as a novel therapeutic modality for cancer in recent years [1,2]. Compared with conventional modalities like surgery and chemotherapy, PTT attracts more interests owing to the non-invasiveness, spatiotemporal controllability and minimal side effects [3]. PTT utilizes photothermal agents (PTAs), which can absorb light energy and convert it into thermal energy, to generate heat and ablate tumor cells upon laser irradiation [4]. PTAs are inorganic or organic nanomaterials with excellent photothermal conversion efficiency (PCE) in near-infrared (NIR) window (650–1350 nm), including precious metal nanoparticles such as Au [5] and Pd [6], carbon-based nanomaterials such as graphene [7] and carbon nanotubes [8], metal sulfide materials such as Ag_2S [9] and CuS [10], polymers such as polydopamine (PDA) [11] or organic dyes such as indocyanine green (ICG) [12]. Generally, inorganic PTAs perform higher PCE and photostability, while the organic

* Corresponding author.
E-mail address: dydszyzf@163.com (Y. Ding).
[1] These authors contributed equally to this work.
Peer review under responsibility of Shenyang Pharmaceutical University.

https://doi.org/10.1016/j.ajps.2021.10.001

PTAs are more bio-compatible and -degradable [13]. Thanks to the rapid development of nanomedicine, nanotechnology is widely applied to overcoming the shortcomings of PTAs. Rational design of nanomedicine could ensure the biostability of the payload and realize targeted delivery and controllable release, thus improving the biocompatibility. For instance, PTAs are modified by biomimetic nanomaterials or shielded in/on protective nanocarriers to promote their biocompatibility or photostability. [14]. Moreover, multifunctional nanosystems are elaborately fabricated to efficiently deliver PTAs, and optimize PTT in cancer treatment [15].

In conventional PTT, the local temperature is elevated to over 50 °C to induce thorough necrosis of tumor cells [16,17]. Nevertheless, such a harsh PTT (hPTT) is not recommended in clinic due to inevitable damage to the surrounding normal tissues and the host antitumor immunity [18,19]. In addition, non-specific heat diffusion induced by hPTT may destruct the vasculature nearby, which hinders the relay delivery of therapeutic agents to the deep tumor site [20]. Therefore, researchers attempt to ablate tumor at a mild temperature (a little higher than physiological temperature, usually 42–45 °C) [21]. Since the temperature gives a positive relationship with the power density and duration of laser irradiation under a certain concentration of PTAs, the mild temperature can be achieved and maintained by manually tuning the parameters of laser irradiation. Of note, a mild laser power density below 0.33 W/cm^2 (for 808 nm laser) or 1 W/cm^2 (for 1064 nm laser) is permitted for safe skin exposure whereas a harsh laser irradiation might cause severe burn to the skin [3]. In clinical investigations, mPTT has only been applied in superficial tumors, including head and neck cancer (NCT00848042) and prostate cancer (NCT02680535), with "AuroShell particles", a kind of gold nanoparticles, utilized as the PTAs. The nanomedicine-based mPTT have achieved appreciable therapeutic efficacy in the studies, accompanied with minimal damage to surrounding healthy tissue. The results validate the promising future of mPTT in clinical practice, but safety and metabolism concerns of the photothermal nanomedicine remain unsolved. Moreover, the application of mPTT in deep-situated tumors is seriously hampered by the tissue penetration of the light source.

Compared to hPTT, mPTT could induce heat stress such as denaturation of proteins and nucleic acid, and ultimately cause apoptosis of tumor cells without the abovementioned adverse effects. However, tumor cells innately response to the external stimuli via a series of defensive mechanisms. Primarily, heat shock response is triggered by heat stress, and then heat shock proteins (HSPs) are produced in abundance to assist in the recovery of the misfolded or denatured proteins, thereby maintain the survival of cells [22]. Besides, autophagy also protects targeted cell by degrading and recycling the impaired organelles when injury occurs [23]. These defensive mechanisms protect normal cells from hyperthermia, yet lead to the thermo-resistance of cancer cells, and greatly compromise the therapeutic efficacy of mPTT. To maximize mPTT efficacy, nanomedicine-based strategies are proposed involving inhibition of HSPs and regulation of autophagy. Upon disruption of heat shock response or autophagy, the thermo-resistance of cancer cells will be reversed, thus potentiating mPTT for ablating thermosensitive tumors.

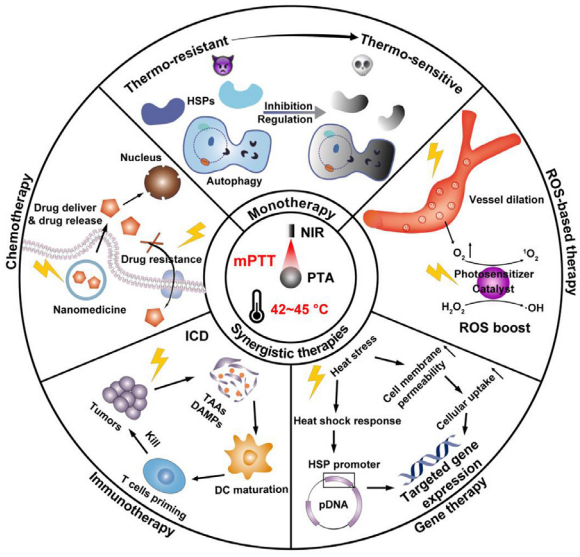

Fig. 1 – Schematic illustration of nanomedicine-potentiated mild PTT as monotherapy or synergizing with other therapeutic modalities for cancer therapy.

Despite great efforts contributed to mPTT promotion, single-mode enhanced mPTT is still insufficient to ablate tumor completely, because the application of PTT exerts limited area of irradiation and depth of penetration, which potentiates the recurrence and metastasis of tumors [24]. Hence, nanomedicine with multiple therapy modalities are combined with mPTT to synergistically enhance antitumor efficacy, and reduce side effects [25]. In this review, we will overview the recent advances in nanomedicine- potentiated mild temperature photothermal therapy of cancer, including strategies for enhancing mPTT and synergistic therapies with mPTT. As shown in Fig. 1, mono mPTT is enhanced by inhibiting HSPs or regulating autophagy to overcome the thermo-resistance of cancer cells. In synergistic therapies, mPTT performs diverse functions including promoting nanomedicine delivery and reversing drug resistance in synergy with chemotherapy, inducing immunogenic cell death (ICD) in synergy with immunotherapy, modulating gene expression in synergy with gene therapy, and boosting reactive oxygen species (ROS) in synergy with ROS-based therapy. At last, we discuss the principle of rationally designed nanomedicine to optimize mPTT in cancer therapy, together with further perspectives in challenges and prospects for clinical translation of nanomedicine-potentiated mPTT.

2. Nanomedicine-potentiated strategies for enhancing single-mode mPTT

Mild hyperthermia could pose moderate threat to cancer cells, but a series of defensive mechanisms would attenuate the efficacy of mPTT, mainly including heat shock response and autophagy. Heat shock response is an evolutionarily conserved adaptive process upon proteotoxic stress

conditions such as hyperthermia. Once perceiving stress, heat shock factor 1 (HSF-1) is activated and binds to the heat shock element, followed by transcription of heat shock proteins (HSPs). As molecular chaperones, HSPs play a vital role in cellular protein homeostasis, which is characterized by normal expression of nascent proteins and restored function of impaired proteins [26]. Apart from heat shock response, autophagy is also an important self-protective pathway for cellular metabolic homeostasis. During the autophagy process, microtubule-associated protein 1 light chain 3 I (LC3 I) is recruited onto the membrane of the autophagosome and transforms into LC3 II, marking the maturation of autophagosome. The autophagosome phagocytizes damaged organelles as well as aged proteins and then fuses with lysosome. The subsequently formed autolysosome degrades the internalized contents into nutrient substances for recycle. By virtue of autophagy, cells can avoid accumulation of harmful metabolite under stress and renew themselves for prolonged survival [27]. Unfortunately, these antiapoptotic and cytoprotective mechanisms endow cancer cells with thermo-resistance and have become an obstacle for effective mPTT [28]. To this end, strategies for inhibition of HSPs and regulation of autophagy are prompted to overcome thermo-resistance of tumor and magnify the efficacy of mPTT.

2.1. *Nanomedicine-potentiated HSPs inhibition for magnifying mPTT efficacy*

Among the HSPs family, HSP70 and HSP90 with molecular weight around 70 kDa and 90 kDa respectively, are essential and mostly studied because they are the major molecular chaperones assisting cancer cells in maintaining the activities of key client proteins for survival under heat stress. Hence, various strategies for HSPs inhibition are developed to overcome the thermo-resistance, including small molecular inhibitors, HSPs-targeting gene therapeutic agents, ferroptosis and starvation therapy (Table 1). To date, plenty of small molecular inhibitors have been found to effectively target and inhibit HSP70 or HSP90. Yang et al. developed a family of poly (vinylpyrrolidone) (PVP) protected metal ion-quercetin (Qu) coordination nanomedicines (Qu-MP) [29]. Quercetin is a natural product exhibiting activities of ROS-elimination, anti-inflammation and HSP70 inhibition (Fig. 2A). Among the family of Qu-MP, Qu-Fe^{II}P was the typical example with the topmost PCE, which ablated tumor without causing thermal and inflammatory damage to normal tissues via low-temperature (45 °C) PTT. As shown in Fig. 2B and 2C, nude mice bearing MCF-7 tumors treated with Qu-Fe^{II}P + NIR laser exhibited superior inhibiting effect on the tumor growth than other treatments, contributing to significant tumor ablation without obvious skin burning or other side effects. Simultaneously, the immunofluorescence staining assay and western blot analysis further evidenced that Qu-Fe^{II}P could significantly down-regulate HSP70 expression (Fig. 2D and 2E), contributing to reversion of thermo-resistance and high tumor ablation efficacy upon low-temperature PTT.

Similarly, HSP90 inhibitors are also integrated into nanomedicines to optimize mPTT. Yang et al. fabricated novel PEGylated one-dimensional nanoscale coordination polymers comprising Mn^{2+}, ICG (a mild PTA) and poly-L-histidine-PEG copolymer (pHis-PEG) to load gambogic acid (GA), a natural HSP90 inhibitor [30]. The designed Mn-ICG@pHis-PEG/GA exerted a low-temperature (about 43 °C) PTT in 4T1 tumor-bearing mice upon 808 nm NIR laser irradiation. After 14 d post treatment, the tumor size greatly decreased, demonstrating excellent antitumor efficacy of this mild-temperature PTT strategy. The Mn-ICG@pHis-PEG/GA + NIR induced higher level of apoptosis in tumor compared with NIR or GA-free groups. The GA-mediated down-regulation of HSP90 reduced the thermo-resistance of cancer cells and enabled the enhanced low-temperature PTT for *in vivo* destruction of tumor.

Despite the success of small-molecular HSP inhibitors in mPTT potentiation, the strategies are still limited by low specificity and short-period HSP suppression. Alternatively, small interfering RNA (siRNA) has attracted increasing attention recently due to its specific silence of HSPs at translational level. Ding et al. designed a PEGylated PDA-coated nucleic acid nanogel (PP-NG) assembled with DNA-grafted polycaprolactone, which crosslinked with HSP70-targeting siRNA (siHSP70) [43]. The PDA was introduced as PTA to realize mPTT as well as shielding shell to protect siRNA from enzymolysis. Through HSP70 silencing, the dual-functionalized therapeutic complex PP-NG-siHSP70 was capable of ablating tumor at mild-temperature (42–45 °C). The *in vivo* antitumor efficacy was evaluated on HeLa tumor-bearing mouse, and PP-NG-siHSP70 mediated mPTT could give nearly complete tumor ablation, verifying the therapeutic benefits of HSP silencing.

Recently, the clustered regularly interspaced short palindromic repeats-associated protein 9 system (CRISPR-Cas9) has shared splendid future in gene editing and medical applications due to its simplicity, flexibility, high specificity and efficiency. Chen et al. established a NIR-triggered therapeutic nanoplatform composed of CRISPR-Cas9 ribonucleoprotein (Cas 9 RNP) and chemotherapeutic drug doxorubicin (Dox) loaded on CuS nanoparticles (NPs) and coated with polyethyleneimine (PEI) [46]. The CuS-RNP/Dox@PEI nanocomposites could liberate Cas9 RNP upon photothermal stimulation for the knockout of HSP90α, which further potentiated the photothermal ablation of tumors at a mild temperature of 43 °C (Fig. 3A). The *in vivo* investigation on A375 tumor model suggested the tumor elimination by CuS-RNP/Dox@PEI + NIR treatment (Fig. 3B and 3C). HSP90α staining of tumor sections and T7 endonuclease 1 mismatch detection assay confirmed that the enhanced mPTT efficacy was mainly ascribed to the knockout of HSP90α (Fig. 3D and 3F).

Apart from the above genetic solutions, endogenic active radicals such as lipid peroxides (LPO) and ROS are generally recognized to devitalize HSPs with high efficiency. A newly discovered cell death form ferroptosis is characterized by disruption of cellular redox homeostasis and excessive generation of LPO and ROS [53]. The LPO could spontaneously form aldehyde degradation products, which crosslink primary amines of proteins to destruct their structure and function. Additionally, the highly reactive LPO could propagate further production of plentiful ROS to react with proteins. Therefore, inducing ferroptosis is a potential strategy for HSPs

Table 1 – Nanomedicine-potentiated strategies for enhancing mPTT.

Strategy	Nanomedicine	Therapeutic agent	Target	Therapeutic temperature	Ref.
Small molecular inhibitors	- Qu-Fe^{II}P	Quercetin	HSP70	45 °C	[29]
	- Mn-ICG@pHis-PEG/GA	GA	HSP90	~43 °C	[30]
	- Smart albumin-based theranostic nanoagent (HSA/dc-IR825/GA)	GA	HSP90	< 45 °C	[31]
	- Thermosensitive GOx/ICG/GA liposomes (GOIGLs)	GA	HSP90	41~42	[22]
	- GO–GA-polymer scaffold	GA	HSP90	45 °C	[32]
	- Bi_2Se_3 hollow nanocubes (HNC-s-s-HA/GA)	GA	HSP90	~ 43 °C	[33]
	- Hollow mesoporous carbon spheres (HMCS-PEG-GA)	GA	HSP90	43 °C	[34]
	- Bovine serum albumin/canine dye 7/geldanamycin nanoparticles (BSA/Cy7-SQ/GM)	GM	HSP90	43 °C	[35]
	- HSP90 inhibitor-delivered flowerlike short-wave infrared nanoprobe (Lu:Nd@NiS_2-EGCG)	Epigallocatechin gallate (EGCG)	HSP90	45 °C	[18]
	- Boron-based multifunctional nanoplatform (Dox-17AAG@B-PEG-cRGD)	17AAG	HSP90	43 °C	[36]
	- Folic acid incorporated SNX-2112 loaed GO nanosheets (GFS)	SNX-2112	HSP90	45 °C	[37]
	- Therapy-induced nanohybrid ICD amplifier (FeOOH@STA/Cu-LDH)	STA-9090	HSP90	40~42 °C	[38]
	- BIIB021-loaded IR780 nano-micelles (PEG-IR780-BIIB021)	BIIB021	HSP90	45 °C	[39]
	- NVP-AUY922 loaded GO/$BaHoF_5$/PEG nanocomposite (GO/$BaHoF_5$/PEG/AUY922)	NVP-AUY922	HSP90	< 45 °C	[40]
	- Multifunctional LY294002-loaded Bi_2S_3–Tween 20 nanotheranostic (Bi_2S_3–Tween 20@LY294002)	LY294002	PI3K (PI3K/Akt/GSK3/HSP) pathway	45 °C	[41]
	- MPEG coated gold nanorod and VER-155,008 micelles (MPEG-AuNR@VER-M)	VER-155,008	HSP70 HSP90	45 °C	[5]
Gene regulation	- Hollow gold nanoshells conjugated with siHSP70 (HGN-siHSP70)	siRNA	HSP70	< 48 °C	[42]
	- PP-NG	siRNA	HSP70	42~45 °C	[43]
	- siRNA-loaded zirconium-ferriporphyrin metal–organic framework nanoshuttle (siRNA/Zr-FeP MOF)	siRNA	HSP70	45 °C	[44]
	- CRISPR-Cas9 nanosystem based on gold nanorods (APACPs)	Cas9 RNP	HSP90α	42 °C	[45]
	- CuS-RNP/Dox@PEI	Cas9 RNP	HSP90α	~ 43 °C	[46]
Ferroptosis	- Pd SAzyme	LPO/ROS	HSPs	42 °C	[6]
Starvation therapy	- GOIGLs	GOx	Glucose	41~42 °C	[22]
	- PHPBNs-S-S-HA-PEG@GOx	GOx	Glucose	45 °C	[47]
	- PDA@hm@CQ@GOx	GOx	Glucose	45 °C	[48]
	- MnO_2 nanosheets (M-NS)	MnO_2	Glucose	46 °C	[49]
	- Rod-shape inorganic biomimetic MnO_2–Au nanozymes (MSNR@MnO_2-Au)	Ultrasmall Au nanoparticle	Glucose	< 50 °C	[50]
	- Gold nanorods/HA/Diclofenac nanosystem (GNR/HA-DC)	DC	Glut1 (Glucose transporters)	< 50 °C	[51]
	- CuS-based NO gas nanogenerator (CuS-PEI/NO-TPP)	NO	Mitochondria	46 °C	[52]

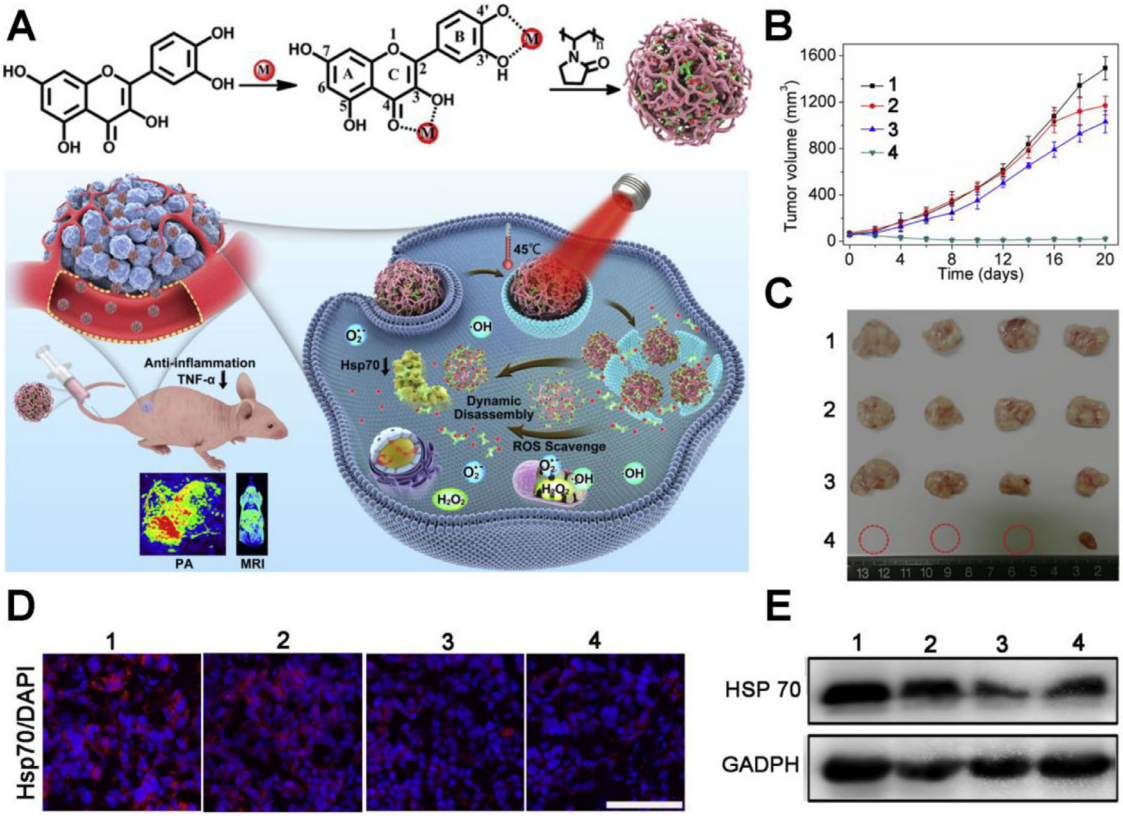

Fig. 2 – A multifunctional nanomedicine to enhance mPTT by HSP70 inhibition. (A) Schematic illustration of the synthesis of Qu-MP, possessing precise diagnosis, excellent mPTT efficacy, ROS scavenge, anti-inflammation, dynamic disassembly and renal clearance ability. (B) Changes of MCF-7 tumor volumes. (C) Images of excised tumors after various treatment ($n = 4$). (D, E) Immunofluorescence staining and western blot of the expression of HSP70 in tumors from mice 36 h after various treatments. 1: PBS, 2: quercetin, 3: Qu-Fe^{II}P, 4: Qu-Fe^{II}P + 808 nm laser (0.5 W/cm^2, 20 min). Scale bar: 200 μm. Reproduced with permission from [29]. Copyright 2019 Elsevier.

devitalization and mPTT enhancement. Chang et al. firstly reported an innovative strategy of ferroptosis-boosted mPTT based on single-atom Pd nanozyme (Pd SAzyme), which exhibited peroxidase and glutathione oxidase mimicking activities and superior photothermal performance [6]. Under 1064 nm laser irradiation, Pd SAzyme raised the temperature mildly (~43 °C) and resulted in ferroptosis of cancer cells for boosting mPTT through HSPs cleavage. The mice treated with Pd SAzyme + 1064 nm laser exhibited remarkable tumor growth suppression effect. The glutathione peroxidase 4 (GPX4, whose inactivation results in ferroptosis) and HSP70 in tumor was detected by immunofluorescence, which further revealed the mechanism that Pd SAzyme markedly down-regulated HSP70 expression via ferroptosis.

Even though HSP70 and HSP90 are crucial for heat shock response, the single-target strategies might lead to incomplete inhibition. Since ATP is an indispensable energy source for protein synthesis including HSPs, intracellular ATP depletion strategies are promising to complete HSPs inhibition and cancer cells sensitization to mild hyperthermia. Zhou et al. designed porous hollow Prussian Blue nanoparticles (PHPBNs) loaded with glucose oxidase (GOx) and coated with PEGylated hyaluronic acid (HA) targeting CD44 [47]. The as-fabricated PHPBNs-S-S-HA-PEG@GOx could deplete ATP via GOx-mediated glucose consumption and generate mild hyperthermia upon NIR laser illumination owing to the high PCE of PHPBNs (Fig. 4A). The combination of tumor starvation and low-temperature PTT of 45 °C yielded advanced therapeutic efficacy of average tumor volume decrease by 32.5% (Fig. 4B) and the highest survival rate against HepG2 tumor (Fig. 4C). The immunofluorescence staining of HSP70 and HSP90 validated the downregulation of HSPs by tumor starvation (Fig. 4D & 4E).

Overall, small molecular inhibitors could target single HSP, multiple HSPs or upstream proteins of HSPs like PI3K and reduce their activities at protein level, while gene therapeutic agents could silence the expression of specific HSP at genetic level with the advantages of high specificity and long-term suppression. However, these two strategies mostly inhibit limited HSP, which may lead to incomplete blockade of HSPs. Fortunately, ferroptosis and starvation therapy potentiate the thorough devitalization of HSPs because they could non-selectively oxidize HSPs by LPO and ROS or block the synthesis of HSPs via ATP depletion, respectively.

2.2. *Nanomedicine-potentiated autophagy regulation for magnifying mPTT efficacy*

Once heat shock response is blocked by HSPs inhibition, cancer cells can still seek bypass for survival. Autophagy is

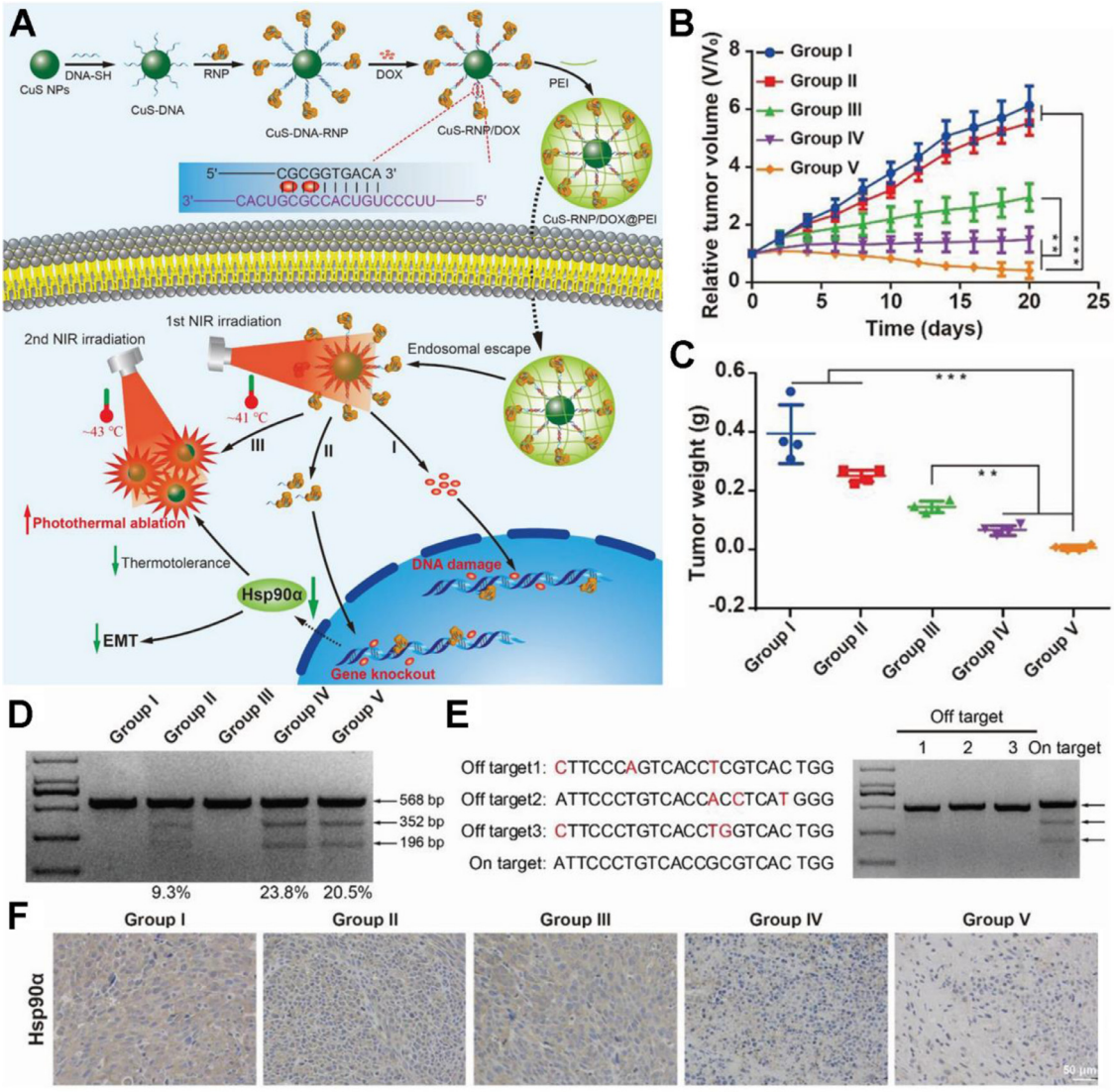

Fig. 3 – A NIR-controlled CRISPR-Cas9 RNP delivery platform for sensitized mPTT via HSP90α knockout. (A) Schematic illustration of stepwise synthesis of CuS-RNP/Dox@PEI and NIR-triggered Cas9-RNP targeting HSP90α delivery for gene editing enhanced mPTT; (B, C) The tumor volumes and weights after treatments of various formulations: (I) PBS (with NIR), (II) CuS-RNP/Dox@PEI (without NIR), (III) CuS NPs (with NIR), (IV) CuS-RNP@PEI (with NIR), and (V) CuS-RNP/Dox@PEI (with NIR); (D) T7 endonuclease 1 mismatch detection assay for indels frequency analysis of tumor regions with various administrations; (E) Off-target effects analysis of tumor tissues after treatment with (IV). Mismatched bases are shown in red. (F) HSP90α staining of tumor tissues. The mean value was analyzed using t-test ($n = 4$, $^{**}P < 0.01$ and $^{***}P < 0.001$). Reproduced with permission from [46]. Copyright 2021 Wiley.

a highly conservative cellular process maintaining cellular homeostasis, but cancer cells rely on autophagy to a great extent for self-healing in resistance to external stress such as starvation and hyperthermia [54]. Hence, inhibiting autophagy is regarded as a potential approach to sensitize cancer cells to mPTT. Gao et al. proposed an enzyme-responsive molecular prodrug (Cyp-HCQ-Yp) containing a photothermal fluorophore cypate (Cyp) and an autophagy inhibitor hydroxychloroquine (HCQ) [55]. The prodrug could release HCQ and self-assemble into a nanoparticle termed as Cyp-Y-NP under sequential catalysis by alkaline phosphatase (ALP) and carboxylesterase (CES). Upon NIR light irradiation, Cyp-Y-NP could achieve improved mild photothermal (less than 44 °C) therapeutic benefits, which was mainly ascribed to HCQ-mediated autophagy inhibition (Fig. 5A). Hematoxylin-eosin (H&E) staining indicated the severe tumor tissue damage in Cyp-HCQ-Yp plus laser treated HepG2 tumor-bearing mice (Fig. 5B), in accordance with the complete tumor growth inhibition (Fig. 5C & 5D). As shown in Fig. 5E, Cyp-HCQ-Yp plus laser induced significant expression and accumulation of the autophagy biomarker (LC3 II), validating the mechanism that HCQ disturbed the fusion

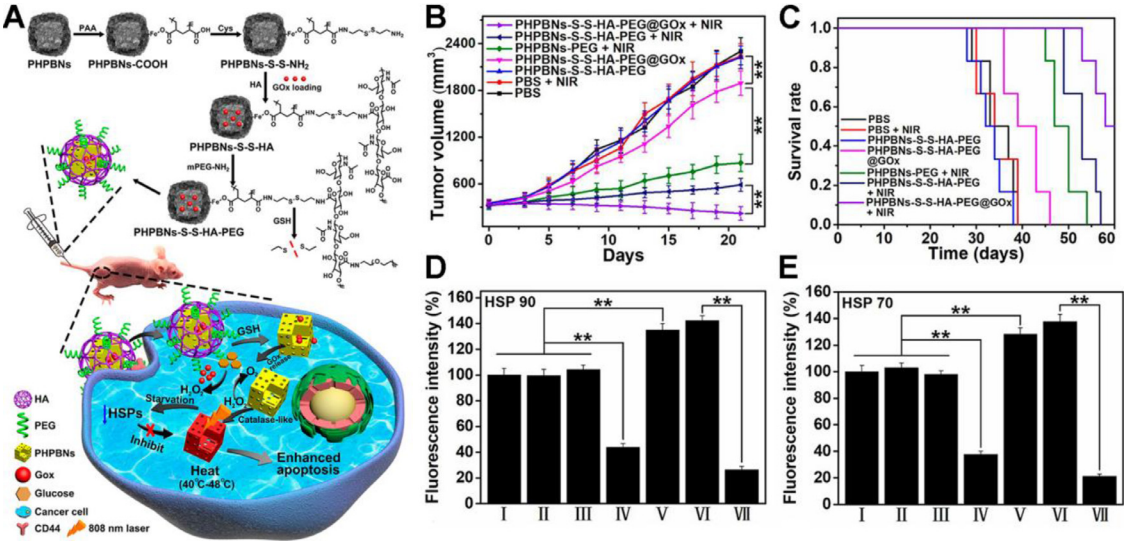

Fig. 4 – A nanosized biocatalyst for energy depletion enhanced mPTT. (A) Schematic illustration of the synthesis of PHPBNs-S-S-HA-PEG@GOx and GOx-mediated starvation synergizing with low-temperature photothermal therapy; (B) Changes of tumor volumes and (C) the survival rate of HepG2 tumor-bearing mice in different groups; (D, E) Quantitative fluorescence analysis of the (E) HSP90 and (F) HSP70 expression after treatment with PBS (I), PBS + NIR (II), PHPBNs-S-S-HA-PEG (III), PHPBNs-S-S-HA-PEG@GOx (IV), PHPBNs-PEG + NIR (V), PHPBNs-S-S-HA-PEG + NIR (VI), and PHPBNs-S-S-HA-PEG@GOx + NIR (VII) for 21 d, respectively. ($n = 6$, $^{**}P < 0.01$). Reproduced with permission from [47]. Copyright 2018 American Chemical Society.

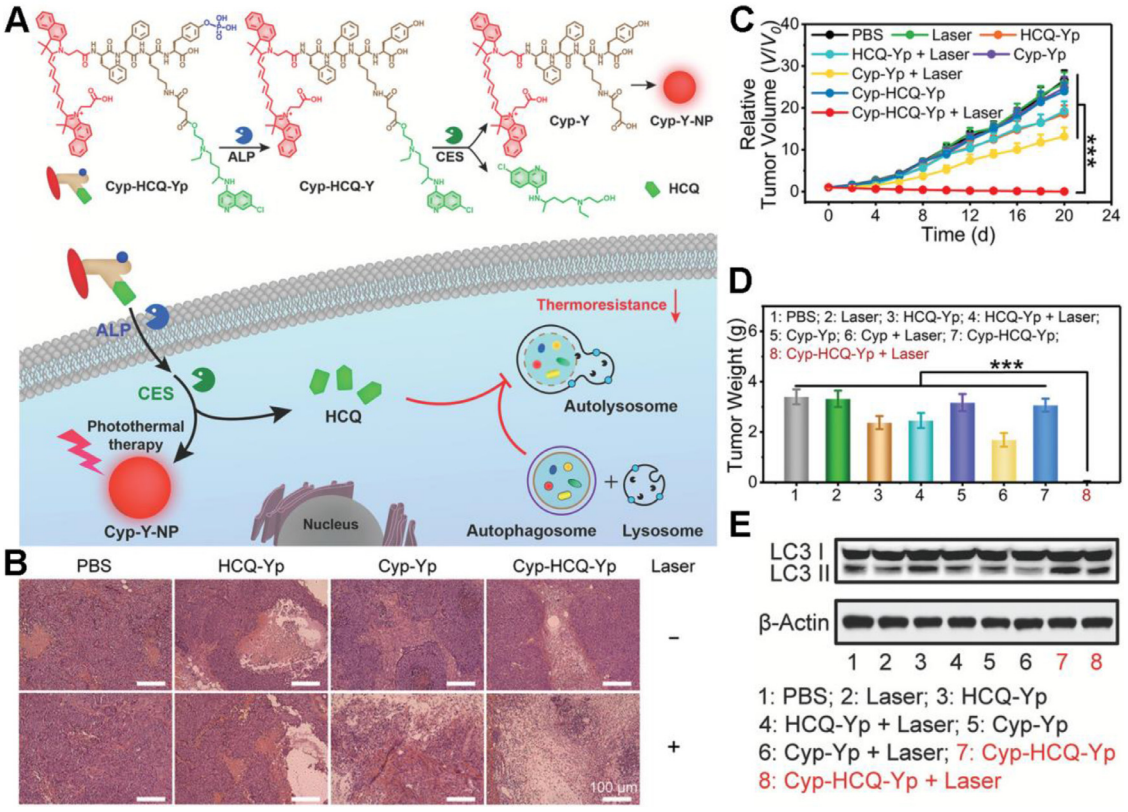

Fig. 5 – A "smart" prodrug for autophagy-inhibited mPTT. (A) Schematic illustration of chemical structures of Cyp-HCQ-Yp and its working mechanism in autophagy-inhibited mPTT; (B) H&E staining of tumor sections collected from the mice at day 20 after different treatments; (C, D) Relative tumor volumes and weights of the excised tumors from the mice after different treatments; (E) The expression levels of LC3 I/II in HepG2 cells as measured by western blotting after different treatments. ($^{***}P < 0.001$). Reproduced with permission from [55]. Copyright 2021 Wiley.

of autophagosome with lysosome and inhibited the laser-triggered autophagy, for ultimate improvement of Cyp-mediated mPTT efficacy.

Inspired by HSPs and autophagy inhibition strategy in overcoming the thermo-resistance of cancer cells, Shao et al. designed a multifunctional rattle-structured nanoparticle with the PDA core autophagy inhibitor chloroquine (CQ) loading and hollow mesoporous silica shell for GOx conjugation [48]. The nanoparticle (PDA@hm@CQ@GOx) integrated therapeutic modalities of low-temperature PTT (~ 45 °C) with energy metabolism regulation and autophagy inhibition for dual-augmented mPTT and trimodal synergistic oncotherapy. PDA@hm@CQ@GOx could significantly down-regulate the expression of HSP70 and HSP90, and obviously increase the expression and accumulation of LC3 II in cytoplasm, indicating the remarkable inhibition of heat shock response and autophagy. PDA@hm@CQ@GOx plus laser resulted in extraordinary *in vivo* tumor regression without any relapse eventually.

Intriguingly, not only can autophagy inhibition attenuate the thermal tolerance of cancer cells, over-activation of autophagy was also reported to boost the efficacy of mPTT. Zhou et al. fabricated a dual peptide decorated melanin-like nanoparticle (PPBR) of PEGylated PDA conjugated with tumor-targeting peptide RGD and autophagy-promoting peptide beclin 1 [56]. The PPBR could up-regulate autophagy via beclin 1 and activate the pathway of autophagic cell death, resulting in an enhanced mPTT around 43 °C. The *in vivo* study was conducted on MBA-MD-231 tumor-bearing mice and the combined autophagy up-regulation associated mPTT exhibited a higher tumor suppression efficacy than mono mPTT or autophagy induction. The highest autophagy level in the PPBR + NIR group was validated by the sharply increased expression of LC3 II protein. These results revealed that the up-regulation of autophagy could remarkably improve the photothermal tumor ablation efficacy.

3. Nanomedicine-promoted synergistic therapies for optimizing mPTT

Though mPTT is capable of ablating primary tumors with the assistance of various strategies reducing the thermal tolerance of cancer cells, the therapeutic effect is too weak to eradicate distant tumors since the photothermal effect can only involve the local areas where PTAs are accumulated and the laser are irradiated. As a result, single-mode mPTT can hardly tackle metastatic tumors even if cancer cells are sensitized to mild hyperthermia. Additionally, mPTT is only applied in superficial tumors in preclinical studies at present because the NIR light has limited depth of penetration. Considering the insufficient efficacy of such a localized therapeutic modality, there is an urgent need to combine mPTT with adjuvant agents to mutually combat relapsed/refractory tumors. In the synergistic therapy, mPTT acts more than thermal ablation, but it also boosts the therapeutic efficacy of other therapeutic modalities. The detailed mechanisms will be discussed about the application of mPTT synergized with chemotherapy, immunotherapy, gene therapy and ROS-based therapy.

3.1. *Nanomedicine-promoted mPTT synergizing with chemotherapy*

Chemotherapy remains the major tool in clinic treatment of cancer. However, the prognosis of patients after chemotherapy is not satisfactory because of systemic toxicity and drug resistance. To overcome the drawbacks caused by chemotherapy, nanomedicine-promoted mPTT would dilate blood vessels to increase blood perfusion and destroy tumor extracellular matrix (ECM), thus enhancing the accumulation of chemotherapeutic drugs at the tumor site and avoiding unnecessary injury to peripheral normal tissue. Upon reaching the target site, nanomedicines are taken into tumor cells and encounter the intracellular barrier such as lysosome capture. Mild hyperthermia destructs the lysosome membrane and triggers escape of drugs from lysosome. What's more, under photothermal stimulation, the connection force between the nanocarrier and drug molecule may be disrupted, thus triggering a rapid release of payloads from the nanocarrier originally. This afterwards overcomes multi-drug resistance as a result of precise shuttling and enhanced accumulation of chemotherapeutics. The mild hyperthermia regulates the drug resistance-related proteins to relieve drug efflux, and recover sensitivity of chemotherapy. Therefore, nanomedicine-promoted mPTT can solve the pivotal problem of *in vivo* delivery of chemotherapeutic drugs and is applied in strategies synergizing with chemotherapy (Table 2).

3.1.1. *mPTT facilitating deep tumor penetration*

Tumor stroma plays an important part in hindering deep penetration of chemical drugs, which comprises ECM, tumor-associated vasculature, stroma cells like cancer-associated fibroblasts (CAFs), tumor-associated macrophages (TAMs) and other cellular or noncellular components. Compared with nonmalignant tissues, tumor tissues turn to be fibrotic and activated, and the ECM gets more rigid and leads to blood vessels embedding into the matrix. Besides, fibroblasts become more proliferative and TAMs are recruited to the solid tumor, contributing to the hard barrier for deep tumor penetration [82].

Nanomedicine-promoted mPTT has been proved to disrupt tumor stroma barrier and dilate tumor blood vessels, resulting in enhanced cellular uptake. Wang et al. designed Gd-hybridized plasmonic Au-nanocomposites to capture Dox (NC-Dox) for multimodal imaging-guided chemotherapy (Fig. 6A) [64]. Upon NIR laser irradiation, the temperature at tumor site reached 42–43 °C, contributing to improved accumulation of NC-Dox in tumor, and drove the trans-vascular transport into the tumor interstitial space. Photoacoustic (PA) imaging was applied to evaluating the *in vivo* infiltration and accumulation enhanced by mPTT. At 6 h after NIR laser irradiation, the nanomedicine showed an enhanced 3.8-fold retention in tumor compared with the unirradiated group (Fig. 6B & 6C). Moreover, the moderate thermal from the plasmonic nanocomposites was confirmed to promote pathological permeability and retention effects. Synchrotron radiation X-ray fluorescence (SR-XRF) mapping was conducted to study the intratumor distribution characteristics of NC-Dox. The major Au and

Table 2 – Nanomedicine-promoted strategies for mPTT synergized with chemotherapy.

Improved chemotherapy efficacy by Mptt	Nanomedicine	PTA	Chemotherapeutic agents	Mechanisms	Ref.
Cellular uptake	- HSA-ICG-PTX	ICG	PTX	- Enhance cell membrane permeability	[25]
	- Zwitterionic polypeptide nanomedicine	AuNRs	Dox		[57]
	- Triple stimuli-responsive polymer–drug conjugate nanoparticles	PDA	Chlorambucil		[58]
	- CuS@BSA-HMONs-Dox	CuS	Dox		[59]
	- PLGA/PPy loaded DTX	Polypyrrole (PPy)	Docetaxel (DTX)		[60]
	- PEGylated AuNRs	AuNRs	HPMA copolymers	- Increase blood perfusion	[20]
	- Gold nanoshell@mesoporous silica nanorod	AuNRs	Gemcitabine	- Destroy dense tumor stroma barrier	[61]
	- TMZ/PSi NPs	Porous silicon (PSi)	Temozolomide (TMZ)	- Improve oxygen supply	[62]
	- PSN–HSA-PTX-IR780	IR780	PTX	- Induce tissue injury	[63]
Drug release	- Au@SiO_2 (Gd)@PDC@HA	Au	Dox	- Disrupt interaction between nanocarrier and drug	[64]
	- CuS@BSA-HMONs-Dox	CuS	Dox		[59]
	- Dox-SWNH/DCA-HPCHS	Single-walled carbon	Dox		[65]
	- aHLP (acid-activated hemolytic polymer)–PDA nanoparticle	PDA	aHLP		[66]
	- Multimodal selenium nanoshell-capped Au@mSiO_2 nanoplatform	Au	Dox		[67]
	- PDA-ALN-SN38	PDA	SN38		[68]
	- PNOC-PDA/NO/Dox	PDA	Dox		[69]
	- Zwitterionic polypeptide nanomedicine	AuNRs	Dox	- Enhance drug diffusion	[57]
	- Ag_2S QD coating with dendritic mesoporous silica (DMSN) loaded with Dox	Ag_2S	Dox		[70]
	- Triple stimuli-responsive polymer–drug conjugate nanoparticles	PDA	Chlorambucil		[58]
	- Gold-nanodot-decorated hollow carbon nanospheres loaded with Dox	Gold-nanodot-decorated hollow carbon	Dox		[71]
	- Thermosensitive Liposomes	Au	Dox	- Trigger disassembly of thermosensitive	[72]
	- Mild-heat-inducible sequentially released liposomal complex	AuNRs	STS		[73]
	- Thermo-sensitive liposome coated gold nanocages with Dox loading	Au	Dox		[74]
	- Gold nanorod-cored biodegradable micelles	AuNRs	Dox		[75]
	- UCNPs@ZrO_2-Ce6/Dox/PCM	Nd^{3+}-doped upconversion nanoparticle	Dox		[76]
	- 5-FU/Cu-LDH@NAB-PTX	Cu	5-FU, PTX		[77]
	- Ag_2S QD coating with dendritic mesoporous silica loaded with Dox	Ag_2S	Dox	- Improve oxygen supply	[70]
	- Melanin coated magnetic nanoparticles	Melanin	Obatoclax (OBX)	- Trigger specific response of NPs	[78]

(*continued on next page*)

Table 2 (*continued*)

Improved chemotherapy efficacy by Mptt	Nanomedicine	PTA	Chemotherapeutic agents	Mechanisms	Ref.
Drug resistance	- MoS_2-PEI-HA/Dox	MoS_2	Dox	- Down-regulate P-gp	[79]
	- Gold-nanodot-decorated hollow carbon nanospheres loaded with Dox	Gold-nanodot-decorated hollow carbon	Dox	- Down-regulate mutant p53, P-gp, MDR-1, IKKa, p-IKKa, p-IκB, p65, p-p65	[71]
	- PNOC-PDA/NO/Dox	PDA	Dox	- Up-regulate HSF-1 trimers	[69]
	- Au@SiO_2 nanoplatform	Au	Dox		[80]
	- Thermo-sensitive liposome coated gold nanocages	Au	Dox	- Down-regulate mutant p53, P-gp, HSF-1	[74]
	- F-Pt-NPs	Pt	Cisplatin	- Facilitate cisplatin uptake - Accelerate GSH depletion - Increase cross-linking of Pt (II) with DNA	[81]

Gd signals of NC-Dox group without laser appeared in the tumor margin. While after mPTT, NC-Dox accumulation at the middle area (1.6–3.2 mm from margin) of tumor increased to about 3.6-fold (Fig. 6D). In addition, NC-Dox extravasated from tumor blood vessels and mainly accumulated in the tumor after irradiation, which was confirmed by staining the blood vessel marker CD31 (Fig. 6E). These results proved that mPTT meditated by plasmonic nanocomposites could remarkably advance the accumulation of nanomedicines at the tumor site and carve out an effective way for chemotherapy.

To evaluate the effect of various heating parameters (temperature and duration) on the intra-tumoral accumulation, Frazier et al. investigated the accumulation altering of water-soluble N-(2-hydroxypropyl)-methacrylamide (HPMA) copolymers under 40, 43, 46 and 49 °C enhanced by gold nanorods (AuNRs) meditated plasmonic PTT [20]. After treatment of laser irradiation for 10 min or 30 min, the moderate temperature of 43 °C led to a larger peak of accumulation at 4 h with the thermal enhancement ratio (TER) of 1.6 compared to the minimal accumulation at 40 °C (TER ~1.2). Interestingly, after the irradiation of 46 °C for 10 min, the accumulation and washout were accelerated from 43 °C groups. With further increase of thermal dose, the tumor vasculature might be damaged for prolonged retention confirmed by histological analyses. This study provided an optimal selection for cancer thermal therapy to maximally enhance polymer accumulation, and meanwhile avoid damage to surrounding tissues.

Apart from the plasmonic meditated mPTT, other PTAs have contributed to the drug delivery as well. Zhao et al. explored the effect of AuNRs meditated mPTT on pancreatic tumor microenvironment (TME) [61]. The group synthesized transferrin (Tf) modified gold nanoshell-coated rod-like mesoporous silica (Tf-GNRS) nanoparticles together with gemcitabine loading (Fig. 7A). According to the real-time multispectral optoacoustic tomography (MSOT), the captured cross-sectional optoacoustic images of live mice demonstrated enhanced signal intensities of hemoglobin (Hb) and oxyhemoglobin (HbO_2) after NIR laser irradiation, which represented increased blood perfusion and oxygen supply (Fig. 7B & 7C). H&E staining sections of MIA-PaCa-2 tumor further proved the elevated blood perfusion after mPTT, resulting in remarkably improved accumulation and penetration of Tf-GNRS at the tumor site (Fig. 7D). As Table 2 summarized, recent related studies have confirmed that mPTT could facilitate drug delivery by increasing blood perfusion and cell membrane permeability, disrupting the dense tumor stroma. Various mechanisms for enhancement of drug accumulation via mPTT may provide multiple ideas to improve chemotherapy.

3.1.2. *mPTT triggering burst drug release*

After entering the blood circulation by intravenous injection, nanomedicines sequentially accumulate and penetrate tumor tissues; and the effective cell endocytose and intracellular drug release are of importance to ensure the completion of drug delivery. As a result, intelligent nanomedicines guided by mPTT are designed to enable accurate release at the tumor site. Structurally, mPTT could disturb the binding force between the nanocarrier and the chemical drugs for on-demand triggering drug. A multifunctional melanin-like nanoparticle was developed for the high encapsulation of 7-ethyl-10-hydroxycamptothecin (SN38) via π-π stacking, which could be dissociated by the mild hyperthermia generated from alendronate-conjugated PDA [68]. After NIR irradiation at 3.6 W/cm^2 for 30 min, there was over 50% SN38 released from the nanoparticle. *In vivo* pharmacodynamic study confirmed that the combination of chemotherapy and mPTT largely suppressed bone tumors and relieved the osteolytic damage of bones. In addition, Qin et al. designed the thermosensitive liposomal complex co-loaded with sodium tanshinone IIA sulfonate (STS) and celastrol (G–T/C–L), and realized controlled drug release upon NIR irradiation at 808 nm [73]. The generated mild heat at around 43 °C

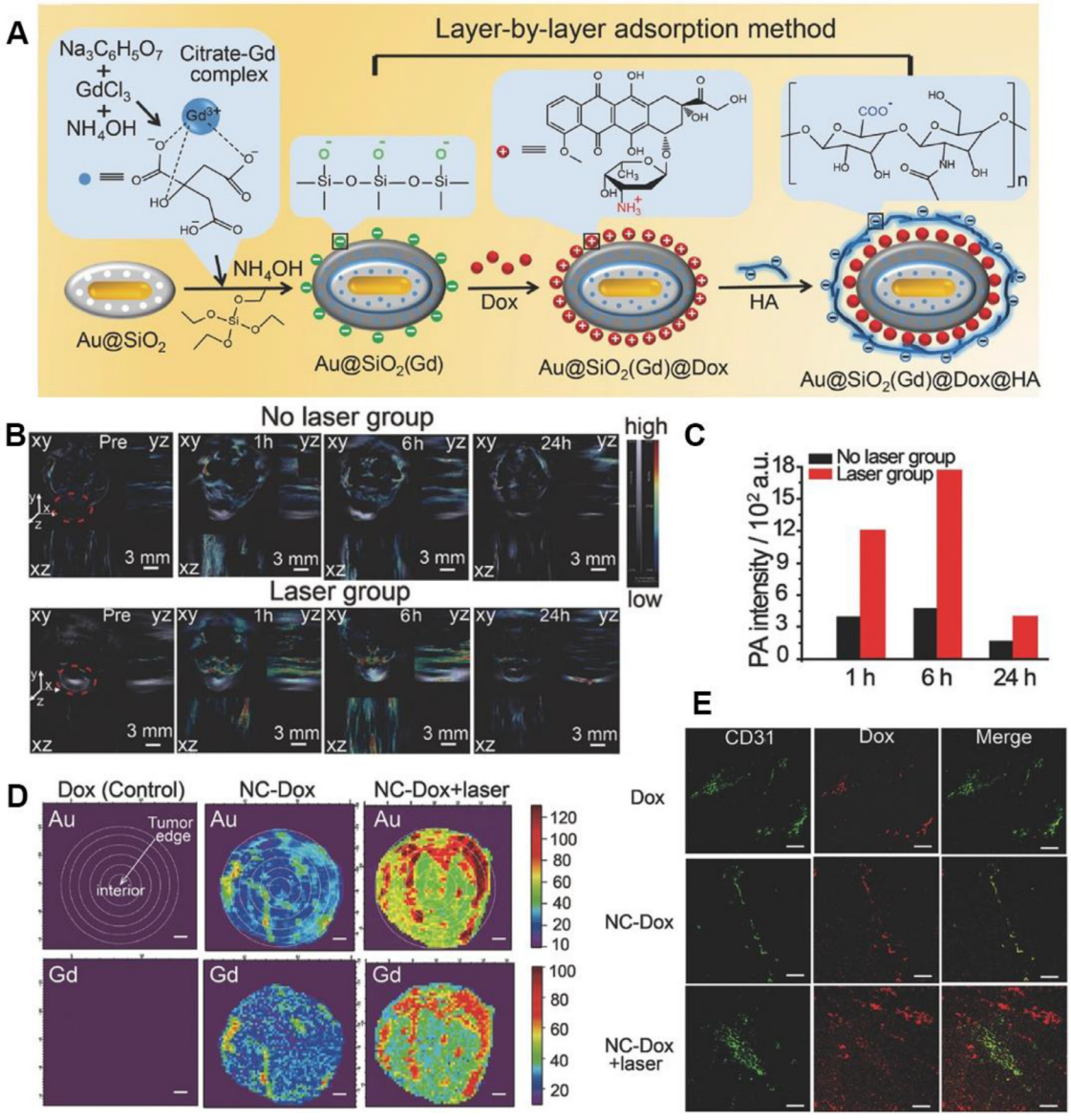

Fig. 6 – Plasmonic Au-nanocomposites induced mPTT to enhance deep penetration in tumor. (A) Synthetic process of Gd-hybridized plasmonic Au-nanocomposites loading high Dox and modified with HA; (B) *In vivo* PA imaging of NCs in no laser group or laser group. The gray section notes the signal intensity of hemoglobin, while the color section notes that of NCs; (C) Mean PA signal intensities of tumor region with or without laser at 1 h, 6 h and 24 h. (D) SR-XRF mapping of Au and Gd of the tumor maximum transverse sections. Scale bar: 1 mm; (E) Immunofluorescence images of the tumor slices staining with CD31. Scale bar: 100 μm. Reproduced with permission from [64]. Copyright 2016 Wiley.

triggered a rapid release of the hydrophilic STS first without damaging to the surrounding normal tissues, which could be attributed to the fact that hydrophilic drug inside the cave was more susceptible for liposomal membrane penetration than that in the lipid bilayer. Moreover, mPTT performed obvious decrease of intra-tumoral collagen area, and down-regulation of abnormally-proliferative tumor blood vessels. The remodeled TME paved the way for celastrol to release and exert the antitumor effect.

3.1.3. *mPTT reversing drug resistance*

Chemotherapy resistance remains a major obstacle for cancer treatment, arising from different mechanisms mainly including overexpression of drug resistance-related proteins like P-glycoprotein (P-gp), which pumps intracellular drug out of the cell, resulting in the deficiency of intracellular uptake and the acceleration of drug efflux. In addition, drugs may associate with complex resistance mechanisms involving intracellular transport obstacle, drug inactivation, increased drug detoxification, etc., which is defined as cascade drug resistance. Recently, the combination of chemotherapy and adjuvant strategies is proved to be effective to overcome drug resistance. Rather than eradicating cancer cells directly through hyperthermia, mPTT is a new tool for overcoming the resistance of drugs, which reduces the expression level of chemo-resistance related proteins, and simultaneously

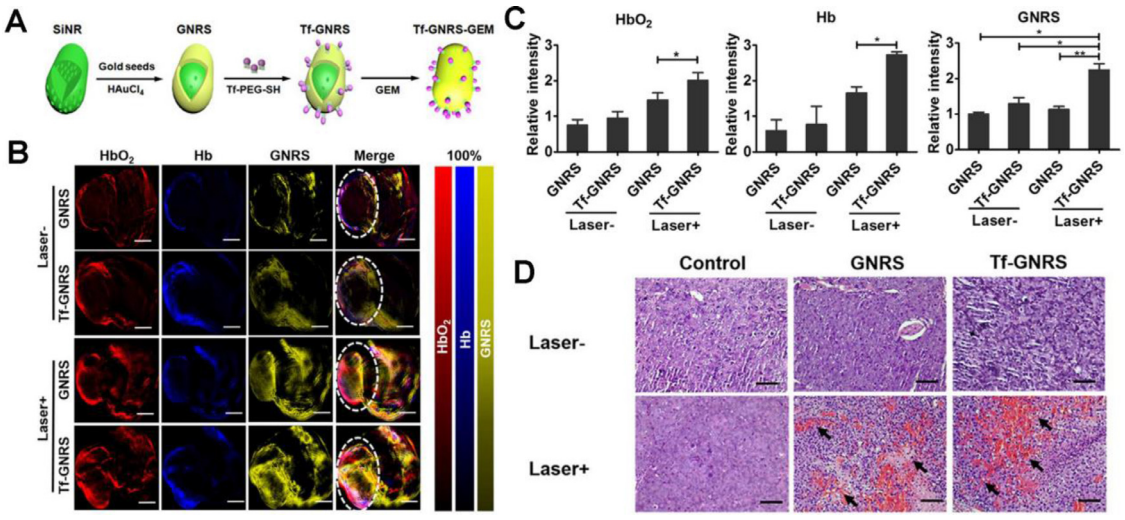

Fig. 7 – GNRS-meditated mPTT for enhancing chemotherapeutics accumulation. (A) Synthetic process of Tf-GNRS; (B) MSOT analysis of GNRS and Tf-GNRS distributions in tumor with or without irradiation (0.5 W/cm^2, 1 min x 3 times, 1 min interval). The white circles mark the tumor regions. Scale bars, 5 mm; (C) Quantitative analysis of the intratumoral signal intensity of GNRS and Tf-GNRS; (D) H&E staining treated with GNRS and Tf-GNRS plus laser irradiation of MIA-PaCa-2 tumor, arrow indicates the blood perfusion of tumor section. Scale bars, 100 μm. (*P < 0.05, **P < 0.01). Reproduced with permission from [61]. Copyright 2017 American Chemical Society.

increases cellular uptake of nanomedicines. Among the chemo-resistance related proteins, HSF-1 plays a vital role in maintaining cellular resistance under stress [82]. Similarly, the mutated form of p53 (mutant p53) proteins ensure the tolerance to chemical drugs in resistant cells [80]. As Fig. 8A showed, a thermo-sensitive liposome coated gold nanocages (LAD) was designed to encapsulate Dox [74]. After administration, the mild heat destroyed the liposomal surface, and induced the higher cellular uptake of Dox in LAD with laser irradiation (LAD+) group (Fig. 8B). The down-regulation of the chemoresistance-related markers (*e.g.*, HSF-1, p53, P-gp) in LAD+ group confirmed that mild heat from LAD was beneficial for reversing drug resistance by increasing the accumulation and sensitivity of Dox (Fig. 8C 8F).

Aside from single mechanism predominated drug resistance, the complex CDR is also involved in chemotherapeutics. Cisplatin, a first-line drug for clinical cancer therapy, is one of the typical drugs that suffer CDR. Generally, cisplatin ablates tumor via covalently binding with DNA to form Pt-DNA adducts. However, abundant intracellular glutathione (GSH) enables rapid detoxification of cisplatin, achieving drug efflux and preventing cisplatin from binding to cellular macromolecules such as DNA. Thus, the CDR process of cisplatin involves complex mechanisms of drug efflux, GSH detoxification and inhibited Pt-DNA adducts formation. Wang et al. complexed a novel hydrophobic photothermal conjugated polymer (DAP-F) with a reduction-sensitive amphiphilic polymer (P1) to form the F-NPs as PTAs. Then, F-NPs were mixed with Pt-NPs encapsulating the prodrug Pt (IV) with P1 to obtain the final nanoparticles (F-Pt-NPs) (Fig. 9A) [81]. The degradation of P1 and reduction of Pt (IV) essentially indicated the GSH depletion. Compared with that at 37 °C, the depletion rate of GSH treated with Pt (IV) and P1 was increased by 10% and 12% respectively under mPTT (43 °C) (Fig. 9B). Furthermore, high-performance liquid chromatography (HPLC) revealed a higher reduction rate of GSH under mild temperature (Fig. 9C). Moreover, F-Pt-NPs showed a significant increase of intracellular uptake by resistant lung cancer cells (A549DDP) under 43 °C (Fig. 9D) and the amount of Pt binding to DNA at 43 °C was 1.18-fold compared with that at 37 °C (Fig. 9E). These evidences revealed that the mild photothermal condition facilitated intracellular uptake of cisplatin, accelerated depletion of GSH to reduce inactivation of cisplatin and increased the cross-linking of Pt (II) with DNA, which ultimately resolved the cascade cisplatin resistance.

3.2. *Nanomedicine-promoted mPTT synergizing with immunotherapy*

Cancer immunotherapy utilizes multi-modalities mainly including cancer vaccines, immunoadjuvants, immune checkpoint blockade (ICB) and adoptive cell therapy to evoke the host immune system and recruit immune cells for tumor eradication [83]. However, the clinical performance of existing cancer immunotherapy is often unsatisfactory due to the poor immune response of patients. It is well known that immunotherapy can only work in immune-active “hot” tumors, while in “cold” tumors, the immune cells are severely restricted by the immunosuppression microenvironment [84 86]. To be specific, they can hardly recognize the tumor cells or reach the tumor site due to the low immunogenicity, abnormal vasculature, dense ECM and high interstitial fluid pressure (IFP) of “cold” tumors. Hence, it is necessary to unleash the constrained immune cells in order to maximize the efficacy of cancer immunotherapy.

As reported, PTT could induce ICD and improve tumor immunogenicity when combined with immunotherapy

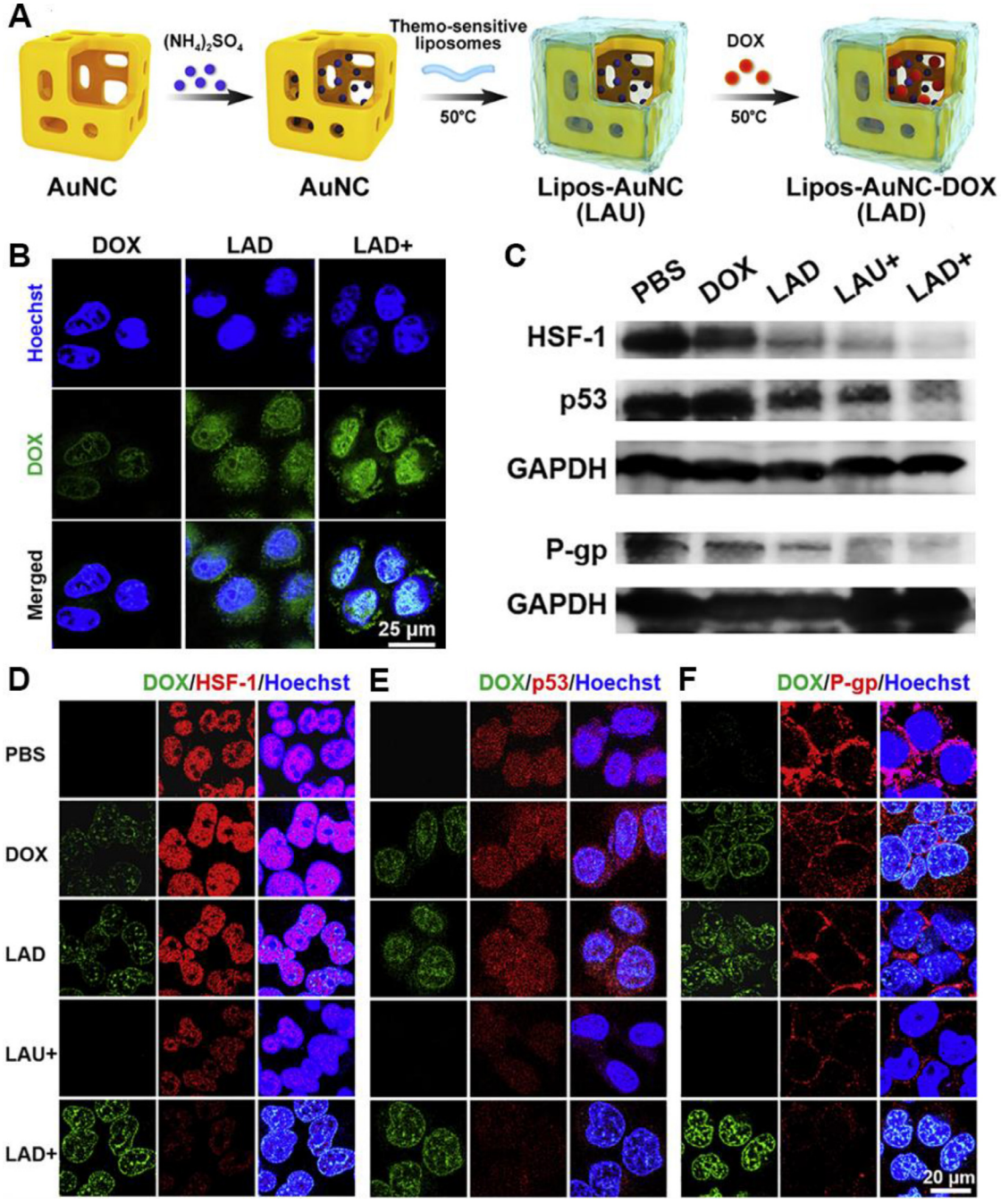

Fig. 8 – Thermo-sensitive liposome-meditated mPTT for reversing Dox resistance. (A) The formation process of LAD; (B) Cellular uptake of Dox, LAD or LAD+ incubated with MCF-7 cells for 1 h. Blue signal: Hoechst, green signal: Dox; (C) Western blot of proteins expression of HSF-1, mutant p53 and P-gp in MCF-7 cells treated with PBS, Dox, LAD, LAU+ and LAD+; (D F) Confocal images of HSF-1 (D), mutant p53 (E) and P-gp (F) expression in MCF-7 cells. "+" indicated treatments with NIR laser irradiation (808 nm, 0.8 W/cm^2, 2 min). Reproduced with permission from [74]. Copyright 2020 Elsevier.

[87]. During ICD, the dying cells release tumor-associated antigens (TAAs) and damage-associated molecular patterns (DAMPs) that can serve as immunoadjuvants to promote the antigen-presenting process. The TAAs are engulfed and processed by antigen presenting cells like dendritic cells (DCs), and transferred to naive T cells in draining lymph nodes; then the stimulated T cells rapidly proliferate and differentiate to kill tumor cells, ultimately achieving immune activation [88]. Nevertheless, hPTT is considered as unfavorable for immunotherapy because hyperthermia might inactivate TAAs, DAMPs and immune cells; and meanwhile, hPTT may destruct the vasculature to hamper the infiltration of immune cells, and cause severe inflammation for attenuation of the antitumor immunity [19,38]. Moreover, Chen et al. demonstrated that mild hyperthermia could increase the blood perfusion, destroy ECM, and reduce

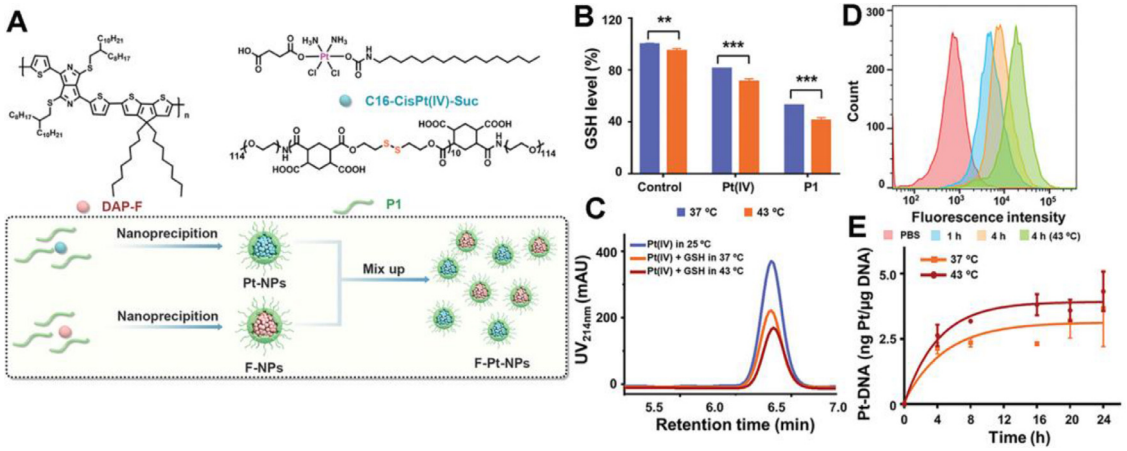

Fig. 9 – F–Pt-NPs-potentiated mPTT for reversing cascade cisplatin resistance. (A) Scheme of the preparation of F-NPs, Pt-NPs and F–Pt-NPs. (B) GSH consumption study via incubating GSH with Pt (IV) or P1 at different temperature for 15 h (*P< 0.001, **P< 0.01). (C) HPLC traces of Pt (IV) treated with GSH (10 x 10^{-3} M) at different temperature for 2 h; (D) Flow cytometry of F–Pt-NPs@Cy5.5 uptake after different treatment; (E) Quantification of Pt-DNA adducts by ICP-MS. Reproduced with permission from [81]. Copyright 2021 Wiley.**

the IFP [89]. Therefore, mPTT is superior to hPTT when combined with immunotherapy owing to the strengths in preserving the antitumor immunity and overcoming the immunosuppressive TME.

Immunoadjuvants are widely applied in cancer vaccines since they can amplify the host immune response to antigens [24,90,91]. mPTT can trigger the release of TAAs, which are regarded as optimal *in situ* cancer vaccines comparable to costly artificial whole tumor antigens. Nanovaccines that combine immunoadjuvants with mPTT-induced *in situ* cancer vaccines are expected to elicit robust antitumor immune response. Liu et al. prepared nanovaccines based on AuNRs decorated with polymerized toll-like receptor 7/8 agonist (polyTLR7/8a) of imidazoquinoline (IMDQ) and PEGylated antigen-trapping peptide of R9-PEG [19]. The designed AuNRs-IMDQ-R9-PEG could generate mild hyperthermia (approximately 45 °C) under 808 nm NIR laser irradiation, and induce tumor ICD. The subsequently released TAAs were captured by PEG-detached AuNRs-IMDQ-R9 to form nanovaccines *in situ*, which could stimulate the host DCs by IMDQ activating TLR7/8 pathways and augment antitumor T-cells responses. As reported, the $CD11c^+CD86^+CD40^+$ DCs in draining lymph nodes were obviously increased in the 4T1 tumor-bearing mice treated with AuNRs-IMDQ-R9-PEG under laser irradiation, which was also confirmed by the elevated concentrations of IFN-γ and IL-12p70, typical cytokines produced by T-cells, NKT cells and DCs, in the serum of mice in this group. Moreover, the AuNRs-based nanovaccines with laser irradiation promoted the differentiation of naive T-cells into tumor-infiltrating $CD3^+CD8^+$ T cells, IFN-γ^+CD8^+ cytotoxic T lymphocytes and $CD94^+CD8^+$ NKT cells, suggesting that mPTT-triggered *in situ* nanovaccines could boost antitumor T-cells responses, and potentiate the treatment of abscopal tumors.

Recently, adoptive cell therapy has been proposed as a novel immunotherapeutic modality, of which chimeric antigen receptor T cell (CAR-T) therapy is the sufficiently studied in treating hematologic malignancies [92]. However, there has not yet any exploration of CAR-T applied in solid tumors mainly because the physical and immune barriers of solid tumors badly hinder the infiltration and recruitment of CAR-T to the tumor parenchyma [89]. Considering that mPTT could establish an immune-favorable TME for immune cells, it is a feasible strategy to combine mPTT with CAR-T therapy for boosting antitumor immunotherapy. Chen et al. reported a nanoengineered CAR-T biohybrids (CT-INPs) for immunotherapy of solid tumors (Fig. 10A), which were fabricated by a biorthogonal reaction between a nano-photosensitizer (ICG nanoparticles, INPs) and CAR-T, without affecting the original activities of CAR-T [93]. To explore the mechanism of the synergy between mPTT and CAR-T therapy, immunodeficient NOD/SCID mice bearing Raji tumors were intravenously injected with CT-INPs followed by laser irradiation. As shown in Fig. 10B-D, mPTT performance resulted in dilated blood vessels, increased blood perfusion, destroyed ECM and loosened tumor tissue, paving the way for enhanced infiltration and deep penetration of CAR-T into the solid tumors. Furthermore, CT-INPs plus laser significantly elevated the level of chemokines whereby enhanced the recruitment of both CAR-T and endogenous immune effector cells (Fig. 10E, F), by which the secretion of antitumor cytokines was notably promoted as well. Therefore, the nanoengineered CAR-T biohybrids under laser irradiation could effectively remodel the TME and amplify the CAR-T-based immunotherapy of solid tumors via breaking through the physical and immune dual-barriers.

The strategy of ICB has achieved great success with an increasing number of immune checkpoint inhibitors coming into the market in recent years, but it still suffers from the dilemma of poor response when treating immunologically "cold" tumors [94]. Although mPTT could convert the "cold" tumor into "hot" tumor, it exhibits confined effects on the residual tumor cells including abscopal tumors, let alone

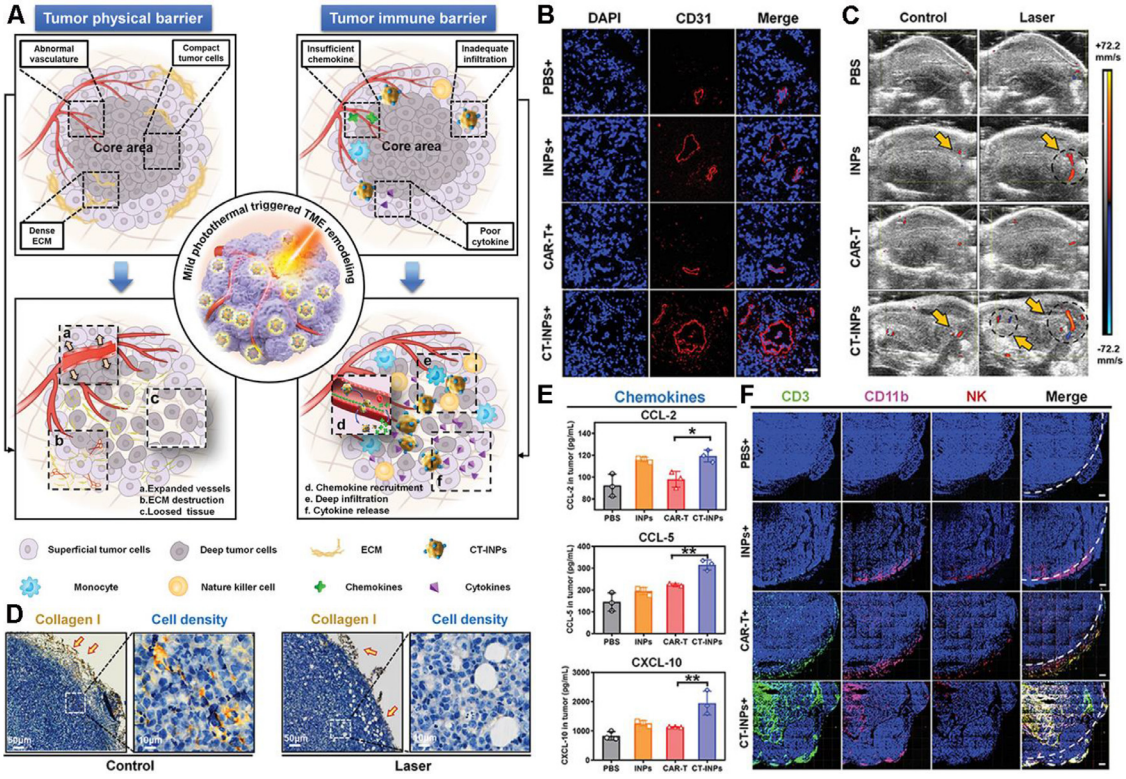

Fig. 10 – Nanoengineered CAR-T biohybrids for solid tumor immunotherapy with TME remodeling by mPTT. (A) Schematic illustration of boosted CAR-T immunotherapy by mPTT-mediated breaking of physical and immune barriers; (B) Immunofluorescence imaging of anti-CD31-APC staining tumor vasculature after mPTT treatment; (C) Ultrasound imaging of tumor blood perfusion after mPTT treatment; (D) Collagen I-represented ECM and cell density analysis in tumor sections after mPTT treatment; (E) Enzyme linked immunosorbent assay (ELISA) analysis of chemokines (CCL-2, CCL-5, and CXCL-10); (F) Immunofluorescence imaging of CT-INPs and endogenous immune cells in tumor tissues ($n = 3$). Sections were stained as blue for nucleus, green for CAR-T, pink for monocytes, and red for NK cells, respectively. Tumor margin was outlined by white dotted line. (Scale bars: 300 μm, *$P < 0.05$, **$P < 0.01$). Reproduced with permission from [93]. Copyright 2021 Wiley.

tumor cells that can upregulate self-protective proteins like immune checkpoints to resist hyperthermia. In this situation, strategies combining mPTT with ICB are of great promise in treating "cold" tumors [95–99]. Huang et al. proposed a combined all-in-one and all-in-control strategy termed as symbiotic mild photothermal-assisted immunotherapy (SMPAI), which utilized a thermosensitive lipid gel (LG) depot to load a PTA (IR820) and an anti-programmed death-ligand 1 antibody (aPD-L1) [100]. The developed aPD-L1/I@LG could generate a mild heat by NIR irradiation on IR820 to trigger the reversible gel-to-sol phase transition for the controllable release of aPD-L1. The activation of systemic immune response increased the tumor-infiltrating lymphocytes and simultaneously upregulated the expression of PD-L1 on tumor cells, thus realizing the SMPAI strategy. After treatment with aPD-L1/I@LG plus NIR irradiation, the 4T1 tumor-bearing BALB/c mice shared a significantly increased population of $CD8^+$ *T* cells and $CD4^+$ *T* cells together with decreased frequency of regulatory T cells (Tregs) and myeloid-derived suppressor cells (MDSCs) in the primary tumors and spleen, indicating that SMPAI strategy could sensitize "cold" tumors with low immunogenicity and few tumor-infiltrating lymphocytes to ICB by promoting T-cells response, and reversing the immunosuppressive microenvironment.

3.3. *Nanomedicine-promoted mPTT synergizing with gene therapy*

Gene therapy could directly regulate the upstream genetic information of the target proteins by gene therapeutic agents [101]. However, the applications of gene therapy are hampered by the intrinsic instability, cytomembrane impermeability, and nonselective transfection of nucleic acid molecules. Encouragingly, numerous nanocarriers are designed to solve the obstacles of gene therapeutics delivery [102]. Nanomedicine-mediated mPTT is reported to enhance the endocytosis of oncolytic adenovirus facilitating the viral transfection [103]. Moreover, given the hyperthermia-triggered expression of HSPs, the upstream promotors of HSPs could be utilized as heat-inducible promotors in gene therapeutic agents such as plasmid DNA (pDNA) to implement controllable expression of target genes via mPTT [95,104].

The transfection efficiency remains challenging in gene therapy using nonviral gene vectors. The mPTT could provide a potential solution due to its permeability elevation effect.

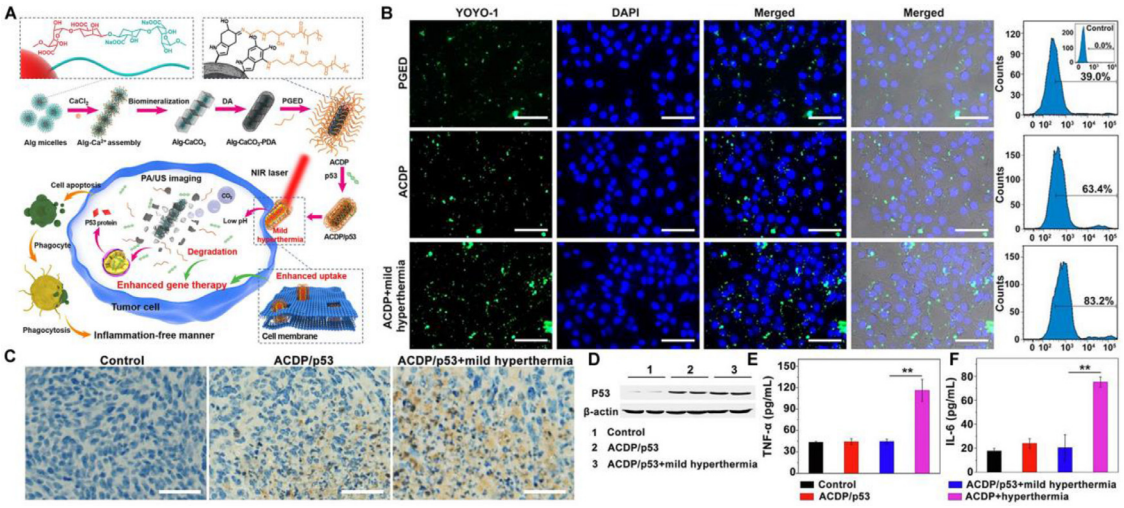

Fig. 11 – Biomineralized calcium carbonate nanohybrids for mPTT-enhanced gene therapy. (A) Schematic illustration of the preparation of the gene carrier and ACDP-mediated mPTT for enhancing gene therapy; (B) Fluorescence images and flow cytometry analysis of 4T1 cells after administration of fluorescently-labeled PGED/pDNA, ACDP/pDNA and ACDP/pDNA with laser irradiation; (C) Immunohistochemical staining of p53 in the tumor tissue. Scale bar: 50 μm; (D) Western blot of P53 protein expression; (E) TNF-α and (F) IL-6 levels in sera of mice after various treatments. Reproduced with permission from [105]. Copyright 2021 Elsevier.

Liu et al. constructed biomineralized calcium carbonate nanohybrids (ACDP) as nanocarriers to deliver antioncogene p53 with PDA deposited on the surface to generate mild heat for p53 transfection efficiency improvement (Fig. 11A) [105]. Fluorescence imaging and quantitative analysis by flow cytometry indicated that mild hyperthermia could increase the permeability of cell membrane and promote the cellular uptake of ACDP/pDNA (Fig. 11B). The *in vivo* antitumor evaluation on 4T1 tumor-bearing mice implied that the mild hyperthermia enhanced the therapeutic efficacy of ACDP/p53. Meanwhile, immunohistochemical staining and western blot assay further verified the transfection promotion of p53 gene by the mild hyperthermia (Fig. 11C & 11D). Moreover, mPTT-enhanced gene therapy hardly induced variations of pro-inflammatory cytokines (TNF-α and IL-6) in sera of mice, whereas conventional hPTT caused inflammatory response due to the cell necrosis (Fig. 11E, F). The results suggested the preferable biosafety of mPTT applications in gene therapy.

After the gene transfection, the precise control of transfected gene activation could maximize the gene therapeutic efficacy. The upstream promotors of HSPs could be integrated into the sequence of target gene and function as a controller of gene expression. The controller-installed therapeutic gene could be activated by the nanomedicine-mediated mPTT. Zhang et al. developed a novel synergistic nanomedicine strategy for gene-directed enzyme prodrug therapy (GDEPT) [106]. The PBDTQ/pCT/Lipid-PEG nanoparticles (PpCTLP NPs) consisted of a NIR-II absorbing semiconducting polymer (PBDTQ) loaded with suicide gene plasmid (pCT), and further incorporated into Lipofectamine 2000. The PpCTLP NPs could exert mild hyperthermia (about 43 °C) and trigger the HSP70 promotor to upregulate the downstream suicide gene expression of cytosine deaminase and herpes simplex virus type-I thymidine kinase (CD-TK), which could convert the prodrugs of 5-fluorocytosine and ganciclovir into their cytotoxic forms, thus realizing GDEPT. The MCF-7 tumor-bearing mice were administrated with PpCTLP NPs and the prodrugs. Under laser irradiation, PpCTLP NPs with prodrugs induced the most remarkable inhibition of tumor growth due to the mPTT-controlled expression of suicide gene and the subsequent conversion of prodrugs to the cytotoxic forms.

3.4. *Nanomedicine-promoted mPTT synergizing with ROS-based therapy*

Excessive ROS could disrupt intracellular signaling and physiological homeostasis, causing the occurrence of diseases [107]. According to previous studies, tumor cells are more vulnerable to ROS compared with normal ones on account of the oxidative stress and the excessive ROS could strike the redox equilibrium and induce apoptosis or necrosis of tumor cells [108–110]. Consequently, ROS-based therapies including radiotherapy (RT), photodynamic therapy (PDT), sonodynamic therapy (SDT) and chemodynamic therapy (CDT) are developed for cancer treatment. Nevertheless, the intratumoral hypoxic environment greatly hinders the therapeutic efficacy of the oxygen-dependent therapy. Numerous nanomedicines are designed to combine mild hyperthermia with ROS-based therapies for hypoxia relief and ROS boost (Table 3).

Despite the diverse therapeutic mechanisms, RT, PDT and SDT are all dependent on oxygen for generating ROS, and thus restricted in the hypoxic TME. As reported, mPTT could dilate blood vessels and increase blood perfusion, contributing to the improved oxygen supply, and is widely exploited to synergize with oxygen-dependent therapies. Cheng et al. designed Gd^{3+}-doped WS_2 nanoflakes with decoration of PEG

Table 3 – Nanomedicine-promoted mPTT synergizing with ROS-based therapy.

Combination therapy	Nanomedicine	PTA	Major effects of mPTT	Ref.
RT	- Multimodal bioimaging-guided nanomedicine	$Gd3^{+}$-doped WS_2	- Improve tumor oxygenation	[111]
	- Core-shell nanomedicine	Ti_3C_2@Au		[112]
	- Bi_2Se_3 hollow nanocubes (HNC-s-s-HA/GA)	Bi_2Se_3	- Raise blood flow	[33]
	- Platinum nanoworm	Pt		[113]
PDT	- Nucleic-acid-driven activatable nanotheranostics	Phthalocyanine photosensitizer (PcS)	- Enhance tumor oxygenation	[114]
	- Zr-FeP MOF	MOF	- Increase ROS production	[44]
	- Lyp-1 modified docetaxel/IR820 co-loaded micelles	IR820		[115]
	- Hypoxia-activated ROS burst liposomes	Ce6		[116]
	- Up-conversion nanoparticle	Fe^{3+} doped MOFs		[117]
	- Pd@Pt-PEG-Ce6	Pt	- Trigger H_2O_2 decomposition to produce oxygen	[118]
	- Au@Rh-ICG-CM	ICG		[119]
	- DiR-hCe6-liposome	Hexylamine conjugated Ce6 (hCe6)	- Increase blood flow	[120]
	- Dual-channel theranostic system	Ce6 & ICG	- Enhance ROS diffusion	[121]
SDT	- Hydrophilic nanomicelles	$AgBiS_2$	- Increase ROS generation	[122]
	- Carbon dot/MXene heterojunctions	Graphitic N-doped carbon dots	- Improve tumor oxygenation	[123]
	- Ultra-small TiN nanodots	TiN		[124]
	- Titanium hydride ($TiH_{1.924}$) nanodots	$TiH_{1.924}$		[125]
CDT	- Layered double hydroxide (LDH) nanoparticles	Cu-LDH/ICG	- Accelerate Fenton reaction	[126]
	- FeOOH@STA/Cu-LDH	Cu-LDH		[38]
	- Hypoxia-activated ROS burst liposomes	Ce6		[116]

corona [111]. As detected by hypoxia marker pimonidazole, the WS_2:Gd^{3+}-PEG + NIR group remarkably reduced hypoxic area compared with the WS_2:Gd^{3+}-PEG treated tumor without NIR irradiation, especially for the circumvascular cells. The results revealed that mPTT could enhance blood flow inside tumor and improve the tumor oxygenation status for RT enhancement. Li et al. also reported a facile preparation via assembly of the phthalocyanine photosensitizer (PcS) and chemotherapeutic mitoxantrone (MA) to form uniform nanomedicines (PcS-MA) (Fig. 12A) [114]. The supramolecular nanostructure could generate singlet oxygen and mild photothermal heating upon irradiation, providing an effective strategy for breaking through the limitations of PDT. Immunofluorescence staining of angiogenesis marker CD31 and hypoxia marker HIF-1α showed that the hypoxic area percentage was decreased from 32.6% to 15.6% after intravenous treatment of PcS-MA + NIR, while the untreated group remained severe hypoxia (Fig. 12B, C). Correspondingly, PcS-MA + NIR shared the superior tumor suppression over the control groups (Fig. 12D).

Similarly, mPTT synergizes with SDT which utilizes sonosensitizers to generate singlet oxygen, by improving blood flow in tumors and alleviating hypoxia for boosting antitumor efficacy. Liu's group prepared titanium hydride ($TiH_{1.924}$) nanodots and ultra-small titanium nitride (TiN) nanodots by liquid-phase exfoliation [124,125]. The $TiH_{1.924}$ and TiN nanodots could serve as both sonosensitizers under ultra-sound and PTAs under NIR irradiation (Fig. 13A & 13D). In ROS staining of 4T1 cells (Fig. 13B & 13E), the laser irradiation group revealed the strongest fluorescence, indicating the ROS generation boost via mPTT-mediated tumor hypoxia improvement. Moreover, immunofluorescence hypoxia staining showed that the nanodot-produced mild heat increased intra-tumoral blood flow and relieved the hypoxia (Fig. 13C & 13F). The results suggested that the mPTT was effective for overcoming SDT resistance in hypoxic tumor.

Differentiated from above-mentioned oxygen-dependent therapies, the therapeutic mechanism for CDT is the activation of Fenton or Fenton-mimicking reaction to produce strong oxidizing hydroxyl free radicals for cytotoxicity. However, CDT fails to achieve significant progress in clinical transformation, mainly due to the poor catalytic activity of Fenton reaction at physiological temperature. Mild heat could elevate temperature at tumor site to accelerate Fenton reaction tumor-specifically, enhancing the antitumor effect of CDT. Tang et al. designed superparamagnetic iron oxide nanoclusters (SPIOCs) to acquire superior Fenton catalyst activity and high PCE [116]. Moreover, chlorin e6, a well-studied photosensitizer was carried on SPIOCs and the complex was further stabilized by hypoxia-responsive poly (metronidazole) liposomes to generate a hypoxia-activated ROS burst nanoparticle. The external light-triggered PDT combined with the endogenous iron oxide nanoclusters-

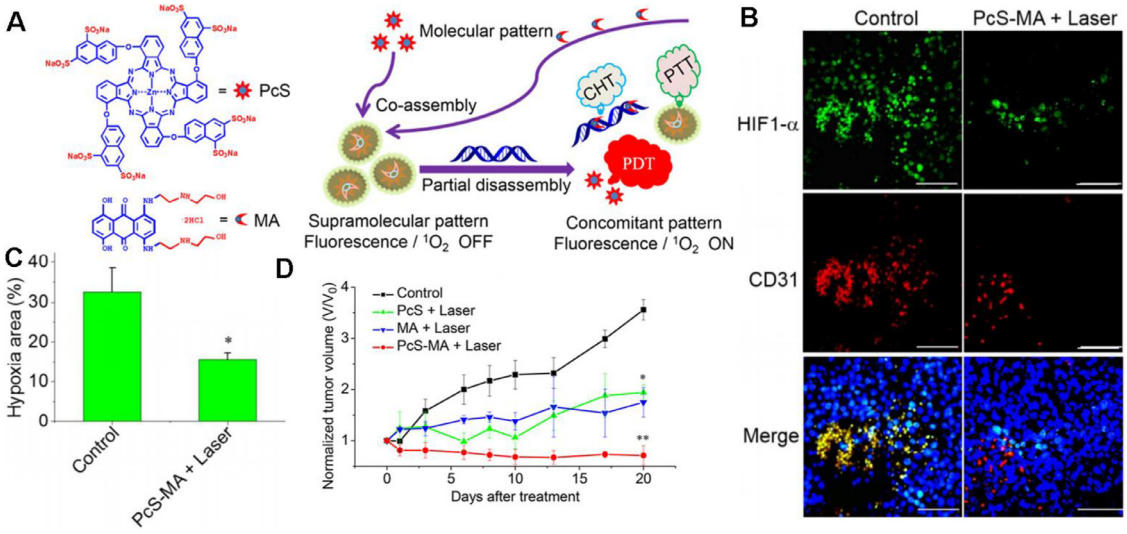

Fig. 12 – PcS-MA nanomedicines-potentiated mPTT synergizing with PDT for tumor ablation. (A) Fabrication of a theranostic nanoparticle via the supramolecular interaction between PcS and MA, nucleic acid-triggered fluorescent imaging, and combinational therapy of PTT, PDT and CH6T; (B) Immunofluorescence images of mice bearing MCF7 tumors after treatment. Tumor hypoxic regions (anti-HIF1-α, green), blood vessels and angiogenesis (anti-CD31, red) and nuclei (DAPI) were detected, respectively. Scale bars indicate 100 μm; (C) Quantitative analysis of hypoxia-positive cells in the immunofluorescence images. Data are expressed as mean ± SEM; (D) The relative tumor volume of the investigated groups, with the data normalized to the volumes at Day 0. The tumors were treated with laser (690 nm, 1 W/cm^2 for 5 min) at 4 h post injection. Data are expressed as mean ± SEM ($n = 5$, *$P < 0.05$, **$P < 0.01$). Reproduced with permission from [114]. Copyright 2018 American Chemical Society.

triggered CDT, are both amplified by mPTT, boosting a mass of ROS for tumor ablation. The hydroxyl radical (•OH) generation was detected by high electron spin resonance (ESR) and methylene blue (MB) depigmentation, and SPIOCs treated group shared the highest •OH level. The results validated the significant mimicking Fenton reaction acceleration by mild hyperthermia (~ 42 °C).

4. Conclusions and perspectives

Nanomedicine-controlled mPTT has received increasing concern in tumor phototherapy owing to its advantages of avoiding damage to the normal tissues over hPTT. However, its therapeutic efficacy is hampered by the thermo-resistance of cancer, which is mainly attributed to the defensive mechanisms including heat shock response and autophagy. To enhance the antitumor efficacy of mPTT, strategies aiming to inhibit HSPs or regulate autophagy are proposed to make cancer cells more susceptible to mPTT. Nevertheless, mono mPTT exerts limited effects mainly due to the complex pathways for tumor proliferation, apoptosis resistance, immune escape, and distant metastases. Thereafter, mPTT is supposed to combine with other potent treatments to synergistically eliminate tumors. Herein, we summarize various strategies for nanomedicine-potentiated mild photothermal oncotherapy, including single-mode mPTT enhancement and mPTT combination with potential therapies of chemotherapy, immunotherapy, gene therapy and ROS-based therapy. Furthermore, we have discussed the underlying mechanisms for the synergistic effects. Primarily, mPTT could elevate the cell membrane permeability, leading to the enhanced cellular internalization of therapeutic agents. The mild hyperthermia likewise contributes to the TME remodeling for lifting restrictions of drug shuttling and immune cell infiltration into the deep tumors. Moreover, mPTT could exogenously trigger the programmed behaviors of nanomedicine, such as rapid drug release, endosomal escape, enzyme or catalyst revitalization [127].

To optimize the efficacy of mPTT in either monotherapy or synergistic therapies, the rational-designed nanomedicines for mPTT are supposed to contain at least two key elements: PTAs and integratable functional modules for enhancing or synergizing mPTT. As the primary element of mPTT, ideal PTAs should possess high PCE against the long-wavelength laser irradiation with skin-endurable intensity for the achievement of preferable mild-temperature. Given that the biosafety of PTA is also a critical concern, the biomimetic materials such as PEG, lipids and proteins are applied to modify the PTA, making it more biocompatible [15]. Secondly, since some PTAs like GO could serve as carriers with extraordinary loading efficiency due to their physicochemical properties, the functional elements could be conjugated through covalent or non-covalent conjugation [128,129]. The integrated nanomedicine for mPTT ought to possess appropriate diameter, charge, morphology, targeting and penetrating ligand for sufficient tumor accumulation and deeply intratumoral distribution of drugs for magnified therapeutic benefits and reduced side effects [130].

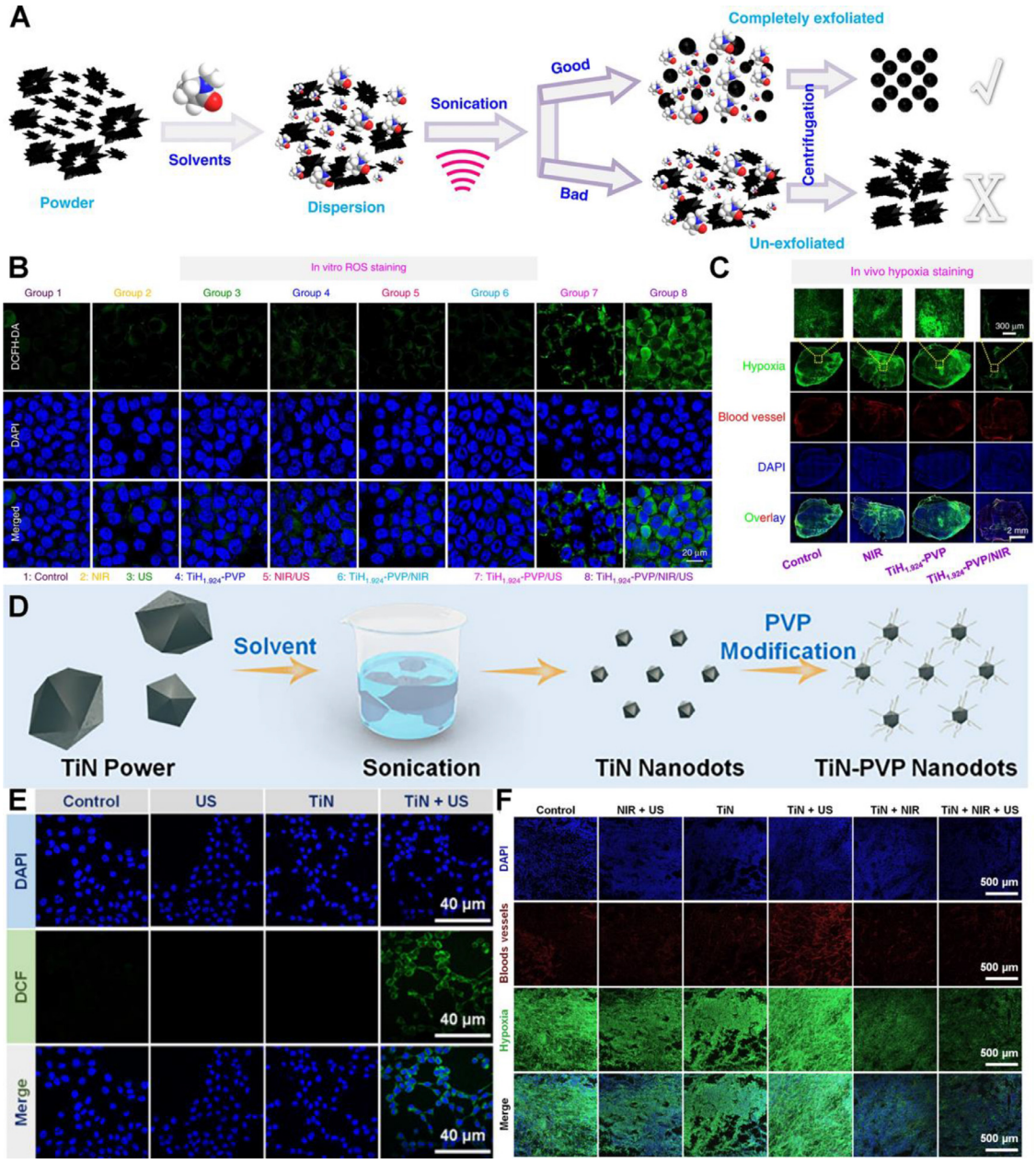

Fig. 13 – $TiH_{1.924}$ and TiN nanodots-potentiated mPTT synergizing with SDT for tumor ablation. (A) Preparation of $TiH_{1.924}$ nanodots via light-phase exfoliation; (B) Fluorescence images of ROS in 4T1 cells treated with $TiH_{1.924}$ nanodots as detected by DCFH-DA probe. The ROS was indicated as green and the nuclei were stained with DAPI and shown as blue; (C) *In vivo* hypoxia staining of tumors treated by $TiH_{1.924}$ nanodots. The blood vessels marker CD31 and hypoxia probe pimonidazole were indicated as red and green respectively, with the nuclei stained by DAPI (blue); (D) Schematic diagram of the fabrication of TiN nanodots and the following decoration; (E) Fluorescence images of ROS in 4T1 cells treated with TiN nanodots; (F) The *in vivo* hypoxia staining of tumors treated by TiN nanodots. (A C) are reproduced with permission from [125]. Copyright 2020 Springer Nature. (D F) are reproduced with permission from [124]. Copyright 2021 Elsevier.

Despite the advanced progress of mPTT, various challenges remain to be solved for clinical applications. To date, the mPTT is merely applied on superficial tumor ablation tumors rather than deep-situated tumors owing to the insufficient penetration depth of NIR-I laser (750-1000 nm). mPTT could only eliminate the tumors efficiently when the tumor volume is below 200 mm^3 in mice according to the previous studies. Given that the NIR-I light decays rapidly as the penetration depth increases, the therapeutic benefits of mPTT are supposed to be limited in very large tumors. Alternatively, the NIR-II (1000–1350 nm) laser has shown superiority of tissue penetration and maximum permissible exposure over the NIR-I laser. Thus, the development of NIR-II-active PTAs would benefit the tumor eradication in deep tissues with preferable safety. The device of light source could also be innovatively manufactured to approach the deep-seated tumors which might refer to the catheter radiofrequency ablation technique. Moreover, multi-photo light source should be employed for the

elimination of deeply located tumors due to the merits of deep tissue penetration and reduced tissue absorption. Although the mPTT is naturally locoregional in tumor treatment, the accidental injury to the surrounding normal cells could barely be avoided. The tumor cell selectivity could be dramatically elevated by the bio-activatable PTAs that are inert in the original form and its photothermal capacity could be activated by the stimuli of tumor microenvironment such as ROS, highly-expressed enzymes [131]. This strategy would endow the mPTT with enhanced safety and anti-tumor efficiency for potential clinical applications. Apart from the tumor cell targeting, the organelle-targeting strategy should be exploited in the design of mPTT nanomedicines for efficient tumor suppression, because the organelles are vulnerable to mild hyperthermia [132,133].

Recently, several novel therapeutic modalities including ion-interference therapy and electrodynamic therapy have shown great promise in tumor treatment, which could be further harnessed in synergistic therapies with mPTT for maximized therapeutic benefits. Notably, despite the extensive researches on the combinational therapies of mPTT and other treatments, the working mechanisms have not been illustrated thoroughly. We suppose that the revelation of detailed mechanisms could guide the rational design of synergistic strategies of mPTT to improve the antitumor efficacy and circumvent potential side effects. In tumor treatment, the ability of mPTT to increase blood flow and loosen extracellular matrix has been validated, which could be applied on the treatment of circulation system diseases like thrombosis. In addition, the mPTT is potential to cure bacterial infections for wound healing acceleration via disturbing the permeability of cytomembrane and cytoderm of bacteria. The photogenerated thermal in mPTT could be utilized for not only the therapeutic purpose but also the medical imaging applications. Therefore, the thermal imaging ought to be highlighted in the further development of mPTT nanomedicine to build the theranostic nanoplatform. The previous studies mainly focus on the various functions of the mPTT nanomedicine, while ignore the accompanied complexity of the nanostructure and manufacture, which might seriously hamper the clinical translation of mPTT. Several principles would help to achieve the balance between the functionality and clinical translation potential of the nanomedicines, including the preference to clinically approved materials in nanostructure fabrication, optimization on the preparation technology, and thorough investigation on safety concerns.

Conflicts of interest

The authors report no conflicts of interest. The authors alone are responsible for the content and writing of this article.

Acknowledgements

The authors gratefully acknowledge the National Natural Science Foundation of China (82073401, 81872819, 82073795). This study was also supported by Young Talent Support Project of Jiangsu Association for Science and Technology (TJ-2021–002), Development Funds for Priority Academic Programs in Jiangsu Higher Education Institutions-Young Talent Program (1131810010), and "Double First-Class" University project (CPU2018GY26).

REFERENCES

[1] Li X, Lovell JF, Yoon J, Chen X. Clinical development and potential of photothermal and photodynamic therapies for cancer. Nat Rev Clin Oncol 2020;17(11):657–74.
[2] Vankayala R, Hwang KC. Near-infrared-light-activatable nanomaterial-mediated phototheranostic nanomedicines: an emerging paradigm for cancer treatment. Adv Mater 2018;30(23):e1706320.
[3] Sun H, Zhang Q, Li J, Peng S, Wang X, Cai R. Near-infrared photoactivated nanomedicines for photothermal synergistic cancer therapy. Nano Today 2021;37:101073.
[4] Xu C, Pu K. Second near-infrared photothermal materials for combinational nanotheranostics. Chem Soc Rev 2021;50(2):1111–37.
[5] Tang XC, Tan LW, Shi K, Peng JR, Xiao Y, Li WT, et al. Gold nanorods together with HSP inhibitor-VER-155008 micelles for colon cancer mild-temperature photothermal therapy. Acta Pharm Sin B 2018;8(4):587–601.
[6] Chang MY, Hou ZY, Wang M, Yang CZ, Wang RF, Li F, et al. Single-atom Pd nanozyme for ferroptosis-boosted mild-temperature photothermal therapy. Angew Chem Int Edit 2021;60(23):12971–9.
[7] Yang K, Zhang SA, Zhang GX, Sun XM, Lee ST, Liu ZA. Graphene in mice: ultrahigh *in vivo* tumor uptake and efficient photothermal therapy. Nano Lett 2010;10(9):3318–23.
[8] Wang C, Xu L, Liang C, Xiang J, Peng R, Liu Z. Immunological responses triggered by photothermal therapy with carbon nanotubes in combination with anti-CTLA-4 therapy to inhibit cancer metastasis. Adv Mater 2014;26(48):8154–8162.
[9] Yang T, Tang YA, Liu L, Lv XY, Wang QL, Ke HT, et al. Size-dependent Ag_2S nanodots for second near-infrared fluorescence/photoacoustics imaging and simultaneous photothermal therapy. ACS Nano 2017;11(2):1848–57.
[10] Li N, Sun Q, Yu Z, Gao X, Pan W, Wan X, et al. Nuclear-targeted photothermal therapy prevents cancer recurrence with near-infrared triggered copper sulfide nanoparticles. ACS Nano 2018;12(6):5197–206.
[11] Huang CL, Zhang L, Guo Q, Zuo YY, Wang NN, Wang H, et al. Robust nanovaccine based on polydopamine-coated mesoporous silica nanoparticles for effective photothermal-immunotherapy against melanoma. Adv Funct Mater 2021;31(18):2010637.
[12] Chen Q, Xu L, Liang C, Wang C, Peng R, Liu Z. Photothermal therapy with immune-adjuvant nanoparticles together with checkpoint blockade for effective cancer immunotherapy. Nat Commun 2016;7:13193.
[13] Cheng L, Wang C, Feng LZ, Yang K, Liu Z. Functional nanomaterials for phototherapies of cancer. Chem Rev 2014;114(21):10869–939.
[14] Xie Z, Fan T, An J, Choi W, Duo Y, Ge Y, et al. Emerging combination strategies with phototherapy in cancer nanomedicine. Chem Soc Rev 2020;49(22):8065–87.
[15] Liu Y, Bhattarai P, Dai Z, Chen X. Photothermal therapy and photoacoustic imaging via nanotheranostics in fighting cancer. Chem Soc Rev 2019;48(7):2053–108.
[16] Gao JB, Wang F, Wang SH, Liu L, Liu K, Ye YC,

et al. Hyperthermia-triggered on-demand biomimetic nanocarriers for synergetic photothermal and chemotherapy. Adv Sci 2020;7(11):1903642.
[17] Luo HH, Wang QL, Deng YB, Yang T, Ke HT, Yang H, et al. Mutually synergistic nanoparticles for effective thermo-molecularly targeted therapy. Adv Funct Mater 2017;27(39):1702834.
[18] Jiang AQ, Liu YX, Ma LY, Mao F, Liu LD, Zhai XJ, et al. Biocompatible heat-shock protein inhibitor-delivered flowerlike short-wave infrared nanoprobe for mild temperature-driven highly efficient tumor ablation. Acs Appl Mater Inter 2019;11(7):6820–8.
[19] Liu X, Su Q, Song H, Shi X, Zhang Y, Zhang C, et al. PolyTLR7/8a-conjugated, antigen-trapping gold nanorods elicit anticancer immunity against abscopal tumors by photothermal therapy-induced *in situ* vaccination. Biomaterials 2021;275:120921.
[20] Frazier N, Robinson R, Ray A, Ghandehari H. Effects of heating temperature and duration by gold nanorod mediated plasmonic photothermal therapy on copolymer accumulation in tumor tissue. Mol Pharmaceut 2015;12(5):1605–14.
[21] Gao G, Sun XB, Liang GL. Nanoagent-promoted mild-temperature photothermal therapy for cancer treatment. Adv Funct Mater 2021;31(25):2100738.
[22] Gao G, Jiang YW, Guo YX, Jia HR, Cheng XT, Deng Y, et al. Enzyme-mediated tumor starvation and phototherapy enhance mild-temperature photothermal therapy. Adv Funct Mater 2020;30(16):1909391.
[23] Zhou ZJ, Yan Y, Hu KW, Zou Y, Li YW, Ma R, et al. Autophagy inhibition enabled efficient photothermal therapy at a mild temperature. Biomaterials 2017;141:116–24.
[24] Zhang Y, He X, Zhang Y, Zhao Y, Lu S, Peng Y, et al. Native mitochondria-targeting polymeric nanoparticles for mild photothermal therapy rationally potentiated with immune checkpoints blockade to inhibit tumor recurrence and metastasis. Chem Eng J 2021;424:130171.
[25] Chen Q, Liang C, Wang C, Liu Z. An imagable and photothermal "abraxane-Like" nanodrug for combination cancer therapy to treat subcutaneous and metastatic breast tumors. Adv Mater 2015;27(5):903–10.
[26] Gomez-Pastor R, Burchfiel ET, Thiele DJ. Regulation of heat shock transcription factors and their roles in physiology and disease. Nat Rev Mol Cell Bio 2018;19(1):4–19.
[27] Levine B, Kroemer G. Autophagy in the pathogenesis of disease. Cell 2008;132(1):27–42.
[28] Yi X, Duan QY, Wu FG. Low-temperature photothermal therapy: strategies and applications. Research 2021;2021:9816594.
[29] Yang GG, Zhou DJ, Pan ZY, Yang J, Zhang DY, Cao Q, et al. Multifunctional low-temperature photothermal nanodrug with *in vivo* clearance, ROS-scavenging and anti-inflammatory abilities. Biomaterials 2019;216:119280.
[30] Yang Y, Zhu WJ, Dong ZL, Chao Y, Xu L, Chen MW, et al. 1D coordination polymer nanofibers for low-temperature photothermal therapy. Adv Mater 2017;29(40):1703588.
[31] Gao G, Jiang YW, Sun W, Guo YX, Jia HR, Yu XW, et al. Molecular targeting-mediated mild-temperature photothermal therapy with a smart albumin-based nanodrug. Small 2019;15(33):1900501.
[32] Bai G, Yuan PY, Cai BL, Qiu XY, Jin RH, Liu SY, et al. Stimuli-responsive scaffold for breast cancer treatment combining accurate photothermal therapy and adipose tissue regeneration. Adv Funct Mater 2019;29(36):1904401.
[33] Song YL, Wang YL, Zhu Y, Cheng Y, Wang YD, Wang SY, et al. Biomodal tumor-targeted and redox-responsive Bi_2Se_3 Hollow nanocubes for MSOT/CT imaging guided synergistic low-temperature photothermal radiotherapy. Adv Healthc Mater 2019;8(16):1900250.
[34] Sun JX, Li YJ, Teng YL, Wang S, Guo J, Wang CC. NIR-controlled HSP90 inhibitor release from hollow mesoporous nanocarbon for synergistic tumor photothermal therapy guided by photoacoustic imaging. Nanoscale 2020;12(27):14775–87.
[35] Wen ZF, Liu FY, Liu GX, Sun QY, Zhang YH, Muhammad M, et al. Assembly of multifunction dyes and heat shock protein 90 inhibitor coupled to bovine serum albumin in nanoparticles for multimodal photodynamic/photothermal/chemo-therapy. J Colloid Interf Sci 2021;590:290–300.
[36] Fu Z, Williams GR, Niu SW, Wu JR, Gao F, Zhang XJ, et al. Functionalized boron nanosheets as an intelligent nanoplatform for synergistic low-temperature photothermal therapy and chemotherapy. Nanoscale 2020;12(27):14739–50.
[37] Deng XY, Guan W, Qing XC, Yang WB, Que YM, Tan L, et al. Ultrafast low-temperature photothermal therapy activates autophagy and recovers immunity for efficient antitumor treatment. Acs Appl Mater Inter 2020;12(4):4265–75.
[38] Li B, Hao GY, Sun B, Gu Z, Xu ZP. Engineering a therapy-induced "immunogenic cancer cell death" amplifier to boost systemic tumor elimination. Adv Funct Mater 2020;30(22):1909745.
[39] Zhang T, Wu BH, Akakuru OU, Yao CY, Sun S, Chen LB, et al. Hsp90 inhibitor-loaded IR780 micelles for mitochondria-targeted mild-temperature photothermal therapy in xenograft models of human breast cancer. Cancer Lett 2021;500:41–50.
[40] Chang X, Zhang MQ, Wang C, Zhang JP, Wu HX, Yang SP. Graphene oxide/$BaHoF_5$/PEG nanocomposite for dual-modal imaging and heat shock protein inhibitor-sensitized tumor photothermal therapy. Carbon N Y 2020;158:372–85.
[41] Song L, Dong XH, Zhu S, Zhang CF, Yin WY, Zhang X, et al. Bi_2S_3-tween 20 nanodots loading PI3K inhibitor, LY294002, for mild photothermal therapy of LoVo cells *in vitro* and *in vivo*. Adv Healthc Mater 2018;7(22):1800830.
[42] Wang ZH, Li SW, Zhang M, Ma Y, Liu YX, Gao WD, et al. Laser-triggered small interfering RNA releasing gold nanoshells against Heat shock protein for sensitized photothermal therapy. Adv Sci 2017;4(2):1600327.
[43] Ding F, Gao XH, Huang XG, Ge H, Xie M, Qian JW, et al. Polydopamine-coated nucleic acid nanogel for siRNA-mediated low-temperature photothermal therapy. Biomaterials 2020;245:119976.
[44] Zhang K, Meng XD, Cao Y, Yang Z, Dong HF, Zhang YD, et al. Metal-organic Framework nanoshuttle for synergistic photodynamic and low-temperature photothermal therapy. Adv Funct Mater 2018;28(42):1804634.
[45] Li XQ, Pan YC, Chen C, Gao YF, Liu XL, Yang KY, et al. Hypoxia-responsive gene editing to reduce tumor thermal tolerance for mild-photothermal therapy. Angew Chem Int Edit 2021;60(39):21200–4.
[46] Chen C, Ma YP, Du SY, Wu YY, Shen PL, Yan T, et al. Controlled CRISPR-Cas9 ribonucleoprotein delivery for sensitized photothermal therapy. Small 2021;17(33):2101155.
[47] Zhou J, Li MH, Hou YH, Luo Z, Chen QF, Cao HX, et al. Engineering of a nanosized biocatalyst for combined tumor starvation and low-temperature photothermal therapy. ACS Nano 2018;12(3):2858–72.
[48] Shao LH, Li YH, Huang FF, Wang X, Lu JQ, Jia F, et al. Complementary autophagy inhibition and glucose metabolism with rattle-structured polydopamine@mesoporous silica nanoparticles for

augmented low-temperature photothermal therapy and *in vivo* photoacoustic imaging. Theranostics 2020;10(16):7273–86.
[49] Tang W, Fan WP, Zhang WZ, Yang Z, Li L, Wang ZT, et al. Wet/sono-chemical synthesis of enzymatic two-dimensional MnO_2 nanosheets for synergistic catalysis-enhanced phototheranostics. Adv Mater 2019;31(19):1900401.
[50] Yang L, Ren C, Xu M, Song Y, Lu Q, Wang Y, et al. Rod-shape inorganic biomimetic mutual-reinforcing MnO_2-Au nanozymes for catalysis-enhanced hypoxic tumor therapy. Nano Res 2020;13(8):2246–58.
[51] Chen WH, Luo GF, Lei Q, Hong S, Qiu WX, Liu LH, et al. Overcoming the heat endurance of tumor cells by interfering with the anaerobic glycolysis metabolism for improved photothermal therapy. ACS Nano 2017;11(2):1419–31.
[52] Wu CC, Wang DQ, Cen MP, Cao LY, Ding Y, Wang J, et al. Mitochondria-targeting NO gas nanogenerator for augmenting mild photothermal therapy in the NIR-II biowindow. Chem Commun 2020;56(92):14491–4.
[53] Xue CC, Li MH, Liu CH, Li YN, Fei Y, Hu Y, et al. NIR-actuated remote activation of ferroptosis in target tumor cells through a photothermally responsive iron-chelated biopolymer nanoplatform. Angew Chem Int Edit 2021;60(16):8938–47.
[54] Mizushima N, Levine B, Cuervo AM, Klionsky DJ. Autophagy fights disease through cellular self-digestion. Nature 2008;451(7182):1069–75.
[55] Gao G, Sun XB, Liu XY, Jiang YW, Tang RQ, Guo YX, et al. Intracellular nanoparticle formation and hydroxychloroquine release for autophagy-inhibited mild-temperature photothermal therapy for tumors. Adv Funct Mater 2021;31(34):2102832.
[56] Zhou Z, Yan Y, Wang L, Zhang Q, Cheng Y. Melanin-like nanoparticles decorated with an autophagy-inducing peptide for efficient targeted photothermal therapy. Biomaterials 2019;203:63–72.
[57] Ding Y, Du C, Qian JW, Dong CM. Zwitterionic polypeptide nanomedicine with dual NIR/reduction-responsivity for synergistic cancer photothermal-chemotherapy. Polym Chem-Uk 2019;10(35):4825–36.
[58] Du C, Ding Y, Qian JW, Zhang R, Dong CM. Achieving traceless ablation of solid tumors without recurrence by mild photothermal-chemotherapy of triple stimuli-responsive polymer-drug conjugate nanoparticles. J Mater Chem B 2019;7(3):415–32.
[59] Li DJ, Zhang T, Min CW, Huang H, Tan DH, Gu WG. Biodegradable theranostic nanoplatforms of albumin-biomineralized nanocomposites modified hollow mesoporous organosilica for photoacoustic imaging guided tumor synergistic therapy. Chem Eng J 2020;388:124253.
[60] Yuan J, Liu JL, Song Q, Wang D, Xie WS, Yan H, et al. Photoinduced mild hyperthermia and synergistic chemotherapy by one-pot-synthesized docetaxel-loaded poly(lactic-co-glycolic acid)/polypyrrole nanocomposites. Acs Appl Mater Inter 2016;8(37):24445–54.
[61] Zhao RF, Han XX, Li YY, Wang H, Ji TJ, Zhao YL, et al. Photothermal effect enhanced cascade targeting strategy for improved pancreatic cancer therapy by Gold nanoshell@mesoporous silica nanorod. ACS Nano 2017;11(8):8103–13.
[62] Zeng XF, Wang Q, Tan X, Jia L, Li YW, Hu MD, et al. Mild thermotherapy and hyperbaric oxygen enhance sensitivity of TMZ/PSi nanoparticles via decreasing the stemness in glioma. J Nanobiotechnol 2019;17(1):47.
[63] Zhao W, Li T, Long Y, Guo R, Sheng QL, Lu ZZ, et al. Self-promoted albumin-based nanoparticles for combination therapy against metastatic breast cancer via a Hyperthermia-induced "platelet bridge". Acs Appl Mater Inter 2021;13(22):25701–14.
[64] Wang J, Liu J, Liu Y, Wang LM, Cao MJ, Ji YL, et al. Gd-Hybridized plasmonic Au-nanocomposites enhanced tumor-interior drug permeability in multimodal imaging-guided therapy. Adv Mater 2016;28(40):8950–8.
[65] Chen DQ, Wang C, Jiang F, Liu Z, Shu CY, Wan LJ. *In vitro* and *in vivo* photothermally enhanced chemotherapy by single-walled carbon nanohorns as a drug delivery system. J Mater Chem B 2014;2(29):4726–32.
[66] Zhu R, Gao F, Piao JG, Yang LH. Skin-safe photothermal therapy enabled by responsive release of acid-activated membrane-disruptive polymer from polydopamine nanoparticle upon very low laser irradiation. Biomater Sci 2017;5(8):1596–602.
[67] Ramasamy T, Ruttala HB, Sundaramoorthy P, Poudel BK, Youn YS, Ku SK, et al. Multimodal selenium nanoshell-capped Au@$mSiO_2$ nanoplatform for NIR-responsive chemo-photothermal therapy against metastatic breast cancer. Npg Asia Mater 2018;10:197–216.
[68] Wang YT, Huang Q, He X, Chen H, Zou Y, Li YW, et al. Multifunctional melanin-like nanoparticles for bone-targeted chemo-photothermal therapy of malignant bone tumors and osteolysis. Biomaterials 2018;183:10–19.
[69] Ding Y, Du C, Qian JW, Dong CM. NIR-responsive polypeptide nanocomposite generates NO gas, mild photothermia, and chemotherapy to reverse multidrug-resistant cancer. Nano Lett 2019;19(7):4362–70.
[70] Li C, Yang XQ, An J, Cheng K, Hou XL, Zhang XS, et al. A near-infrared light-controlled smart nanocarrier with reversible polypeptide-engineered valve for targeted fluorescence-photoacoustic bimodal imaging-guided chemo-photothermal therapy. Theranostics 2019;9(25):7666–79.
[71] Xu LM, Liu J, Xi JB, Li QL, Chang BC, Duan XM, et al. Synergized multimodal therapy for safe and effective reversal of cancer multidrug resistance based on low-level photothermal and photodynamic effects. Small 2018;14(31):1800785.
[72] Ou YC, Webb JA, Faley S, Shae D, Talbert EM, Lin S, et al. Gold nanoantenna-mediated photothermal drug delivery from thermosensitive liposomes in breast cancer. Acs Omega 2016;1(2):234–43.
[73] Qin Y, Liu TT, Guo MF, Liu YP, Liu CY, Chen Y, et al. Mild-heat-inducible sequentially released liposomal complex remodels the tumor microenvironment and reinforces anti-breast-cancer therapy. Biomater Sci 2020;8(14):3916–25.
[74] He HM, Liu LL, Zhang SP, Mb Zheng, Ma AQ, Chen Z, et al. Smart gold nanocages for mild heat-triggered drug release and breaking chemoresistance. J Control Release 2020;323:387–97.
[75] Zhong YN, Wang C, Cheng L, Meng FH, Zhong ZY, Liu Z. Gold nanorod-cored biodegradable micelles as a robust and remotely controllable doxorubicin release system for potent inhibition of drug-sensitive and -resistant cancer cells. Biomacromolecules 2013;14(7):2411–19.
[76] Feng LL, Gai SL, He F, Dai YL, Zhong CN, Yang PP, et al. Multifunctional mesoporous ZrO_2 encapsulated upconversion nanoparticles for mild NIR light activated synergistic cancer therapy. Biomaterials 2017;147:39–52.
[77] Liu JP, Liu K, Zhang LM, Zhong M, Hong TL, Zhang R, et al. Heat/pH-boosted release of 5-fluorouracil and albumin-bound paclitaxel from Cu-doped layered double hydroxide nanomedicine for synergistical chemo-photo-therapy of breast cancer. J Control Release 2021;335:49–58.

[78] Feng T, Zhou L, Wang ZY, Li CX, Zhang YF, Lin J, et al. Dual-stimuli responsive nanotheranostics for mild hyperthermia enhanced inhibition of Wnt/beta-catenin signaling. Biomaterials 2020;232:119709.
[79] Dong XH, Yin WY, Zhang X, Zhu S, He X, Yu J, et al. Intelligent MoS_2 nanotheranostic for targeted and enzyme-/pH-/NIR-responsive drug delivery to overcome cancer chemotherapy resistance guided by PET imaging. Acs Appl Mater Inter 2018;10(4):4271–84.
[80] Wang LM, Lin XY, Wang J, Hu ZJ, Ji YL, Hou S, et al. Novel insights into combating cancer chemotherapy resistance using a plasmonic nanocarrier: enhancing drug sensitiveness and accumulation simultaneously with Localized mild photothermal stimulus of femtosecond pulsed Laser. Adv Funct Mater 2014;24(27): 4229–4239.
[81] Wang LN, Yu YJ, Wei DS, Zhang LP, Zhang XY, Zhang GX, et al. A systematic strategy of combinational blow for overcoming cascade drug resistance via NIR-light-triggered Hyperthermia. Adv Mater 2021;33(20):2100599.
[82] Dong XH, Cheng R, Zhu S, Liu HM, Zhou RY, Zhang CY, et al. A heterojunction structured $WO_{2.9}$-WSe_2 nanoradiosensitizer increases local tumor ablation and checkpoint blockade immunotherapy upon low radiation dose. ACS Nano 2020;14(5):5400–16.
[83] Khalil DN, Smith EL, Brentjens RJ, Wolchok JD. The future of cancer treatment: immunomodulation, CARs and combination immunotherapy. Nat Rev Clin Oncol 2016;13(6):273–90.
[84] Chen QJ, Sun T, Jiang C. Recent advancements in nanomedicine for 'cold' tumor immunotherapy. Nano-Micro Lett 2021;13(1):92.
[85] Huang J, Yang B, Peng Y, Huang JS, Wong SHD, Bian LM, et al. Nanomedicine-boosting tumor immunogenicity for enhanced immunotherapy. Adv Funct Mater 2021;31(21):2011171.
[86] Galon J, Bruni D. Approaches to treat immune hot, altered and cold tumours with combination immunotherapies. Nat Rev Drug Discov 2019;18(3):197–218.
[87] Shang T, Yu X, Han S, Yang B. Nanomedicine-based tumor photothermal therapy synergized immunotherapy. Biomater Sci 2020;8(19):5241–59.
[88] Galluzzi L, Buque A, Kepp O, Zitvogel L, Kroemer G. Immunogenic cell death in cancer and infectious disease. Nat Rev Immunol 2017;17(2):97–111.
[89] Chen Q, Hu QY, Dukhovlinova E, Chen GJ, Ahn S, Wang C, et al. Photothermal therapy promotes tumor infiltration and antitumor activity of CAR T cells. Adv Mater 2019;31(23):1900192.
[90] Chen PM, Pan WY, Wu CY, Yeh CY, Korupalli C, Luo PK, et al. Modulation of tumor microenvironment using a TLR-7/8 agonist-loaded nanoparticle system that exerts low-temperature hyperthermia and immunotherapy for *in situ* cancer vaccination. Biomaterials 2020;230: 119629.
[91] Li Y, He LH, Dong HQ, Liu YQ, Wang K, Li A, et al. Fever-inspired immunotherapy based on photothermal CpG nanotherapeutics: the critical role of mild heat in regulating tumor microenvironment. Adv Sci 2018;5(6):1700805.
[92] Majzner RG, Mackall CL. Clinical lessons learned from the first leg of the CAR T cell journey. Nat Med 2019;25(9):1341–55.
[93] Chen Z, Pan H, Luo YM, Yin T, Zhang BZ, Liao JH, et al. Nanoengineered CAR-T biohybrids for solid tumor immunotherapy with microenvironment photothermal-remodeling strategy. Small 2021;17(14):2007494.
[94] de Miguel M, Calvo E. Clinical challenges of immune checkpoint inhibitors. Cancer Cell 2020;38(3):326–33.
[95] Tang HL, Xu XJ, Chen YX, Xin HH, Wan T, Li BW, et al. Reprogramming the tumor microenvironment through second-near-infrared-Window photothermal Genome editing of PD-L1 mediated by supramolecular gold nanorods for enhanced cancer immunotherapy. Adv Mater 2021;33(12):2006003.
[96] Peng JR, Xiao Y, Li WT, Yang Q, Tan LW, Jia YP, et al. Photosensitizer micelles together with IDO inhibitor enhance cancer photothermal therapy and immunotherapy. Adv Sci 2018;5(5):1700891.
[97] Yang Z, Gao D, Guo XQ, Jin L, Zheng JJ, Wang Y, et al. Fighting immune cold and reprogramming immunosuppressive tumor microenvironment with red blood cell membrane-camouflaged nanobullets. ACS Nano 2020;14(12):17442–57.
[98] Guo MY, Zhang X, Liu J, Gao F, Zhang XL, Hu XH, et al. Few-layer bismuthene for checkpoint knockdown enhanced cancer immunotherapy with rapid clearance and sequentially triggered one-for-all strategy. ACS Nano 2020;14(11):15700–13.
[99] Yu Q, Tang X, Zhao W, Qiu Y, He J, Wan D, et al. Mild hyperthermia promotes immune checkpoint blockade-based immunotherapy against metastatic pancreatic cancer using size-adjustable nanoparticles. Acta Biomater 2021;13:18.
[100] Huang LP, Li YN, Du YN, Zhang YY, Wang XX, Ding Y, et al. Mild photothermal therapy potentiates anti-PD-L1 treatment for immunologically cold tumors via an all-in-one and all-in-control strategy. Nat Commun 2019;10:4871.
[101] High KA, Roncarolo MG. Gene Therapy. New Engl J Med 2019;381(5):455–64.
[102] Kulkarni JA, Witzigmann D, Thomson SB, Chen S, Leavitt BR, Cullis PR, et al. The current landscape of nucleic acid therapeutics. Nat Nanotechnol 2021;16(6):630–43.
[103] Jung BK, Lee YK, Hong J, Ghandehari H, CO Yun. Mild hyperthermia induced by gold nanorod-mediated plasmonic photothermal therapy enhances transduction and replication of oncolytic adenoviral gene delivery. ACS Nano 2016;10(11):10533–43.
[104] Liu YJ, Shu GM, Li X, Chen HB, Zhang B, Pan HZ, et al. Human HSP70 promoter-based prussian blue nanotheranostics for thermo-controlled gene therapy and synergistic photothermal ablation. Adv Funct Mater 2018;28(32):1802026.
[105] Liu YN, Yu BR, Dai XG, Zhao NN, Xu FJ. Biomineralized calcium carbonate nanohybrids for mild photothermal heating-enhanced gene therapy. Biomaterials 2021;274:120885.
[106] Zhang X, Yang YQ, Kang TY, Wang J, Yang G, Yang YM, et al. NIR-II absorbing semiconducting polymer-triggered gene-directed enzyme prodrug therapy for cancer treatment. Small 2021;17(23):2100501.
[107] Zhou ZJ, Ni KY, Deng HZ, Chen XY. Dancing with reactive oxygen species generation and elimination in nanotheranostics for disease treatment. Adv Drug Deliver Rev 2020;158:73–90.
[108] Ming L, Li S, Brooks M, Evelyn J, Zhu Y, Buschhaus JM, et al. Targeting breast cancer stem cell state equilibrium through modulation of redox signaling. Cell Metab 2018;28(1):69–86.
[109] Wang P, Liang C, Zhu J, Yang N, Jiao A, Wang W, et al. Manganese-based nanoplatform as metal ion-enhanced ROS generator for combined chemodynamic/photodynamic therapy. Acs Appl Mater Inter 2019;11(44):41140–7.

[110] Guan X, Yin HH, Xu XH, Xu G, Zhang Y, Zhou BG, et al. Tumor metabolism-engineered composite nanoplatforms potentiate sonodynamic therapy via reshaping tumor microenvironment and Facilitating electron-Hole pairs' separation. Adv Funct Mater 2020;30(27):2000326.
[111] Cheng L, Yuan C, Shen SD, Yi X, Gong H, Yang K, et al. Bottom-up synthesis of metal-ion-doped WS_2 nanoflakes for cancer theranostics. ACS Nano 2015;9(11):11090–101.
[112] Tang WT, Dong ZL, Zhang R, Yi X, Yang K, Jin ML, et al. Multifunctional two-dimensional core-shell MXene@Gold nanocomposites for enhanced photo-radio combined therapy in the second biological Window. ACS Nano 2019;13(1):284–94.
[113] Ma QX, Cheng L, Gong F, Dong ZL, Liang C, Wang MY, et al. Platinum nanoworms for imaging-guided combined cancer therapy in the second near-infrared window. J Mater Chem B 2018;6(31):5069–79.
[114] Li X, Yu S, Lee D, Kim G, Lee B, Cho Y, et al. Facile supramolecular approach to nucleic-acid-driven activatable nanotheranostics that overcome drawbacks of photodynamic therapy. ACS Nano 2018;12(1):681–8.
[115] Li WT, Peng JR, Tan LW, Wu J, Shi K, Qu Y, et al. Mild photothermal therapy/photodynamic therapy/chemotherapy of breast cancer by Lyp-1 modified docetaxel/IR820 co-loaded micelles. Biomaterials 2016;106:119–33.
[116] Tang XL, Wang Z, Zhu YY, Xiao H, Xiao Y, Cui S, et al. Hypoxia-activated ROS burst liposomes boosted by local mild hyperthermia for photo/chemodynamic therapy. J Control Release 2020;328:100–11.
[117] Yang D, Xu JT, Yang GX, Zhou Y, Ji HJ, Bi HT, et al. Metal-organic frameworks join hands to create an anti-cancer nanoplatform based on 808 nm light driving up-conversion nanoparticles. Chem Eng J 2018;344:363–74.
[118] Wei JP, Li JC, Sun D, Li Q, Ma JY, Chen XL, et al. A novel theranostic nanoplatform based on Pd@Pt-PEG-Ce6 for enhanced photodynamic therapy by modulating tumor hypoxia microenvironment. Adv Funct Mater 2018;28(17):1706310.
[119] Wang JP, Sun JY, Hu W, Wang YH, Chou TM, Zhang BL, et al. A porous Au@Rh bimetallic core-shell nanostructure as an H_2O_2-driven oxygenerator to alleviate tumor hypoxia for simultaneous bimodal imaging and enhanced photodynamic therapy. Adv Mater 2020;32(22):2001862.
[120] Feng LZ, Tao DL, Dong ZL, Chen Q, Chao Y, Liu Z, et al. Near-infrared light activation of quenched liposomal Ce6 for synergistic cancer phototherapy with effective skin protection. Biomaterials 2017;127:13–24.
[121] Wang C, Chen SQ, Yu FY, Lv JH, Zhao R, Hu FQ, et al. Dual-channel theranostic system for quantitative self-indication and low-temperature synergistic therapy of cancer. Small 2021;17(10):2007953.
[122] Cheng K, Zhang RY, Yang XQ, Zhang XS, Zhang F, An J, et al. One-for-all nanoplatform for synergistic mild cascade-potentiated uUltrasound therapy induced with targeting imaging-guided photothermal therapy. Acs Appl Mater Inter 2020;12(36):40052–66.
[123] Geng BJ, Xu S, Shen LX, Fang FL, Shi WY, Pan DY. Multifunctional carbon dot/MXene heterojunctions for alleviation of tumor hypoxia and enhanced sonodynamic therapy. Carbon N Y 2021;179:493–504.
[124] Wang X, Wang X, Yue Q, Xu H, Zhong X, Sun L, et al. Liquid exfoliation of TiN nanodots as novel sonosensitizers for photothermal-enhanced sonodynamic therapy against cancer. Nano Today 2021;39:101170.
[125] Gong F, Cheng L, Yang NL, Gong YH, Ni YW, Bai S, et al. Preparation of $TiH_{1.924}$ nanodots by liquid-phase exfoliation for enhanced sonodynamic cancer therapy. Nat Commun 2020;11(1):3712.
[126] Sun L, Wang J, Liu J, Li L, Xu ZP. Creating structural defects of drug-free copper-containing layered double hydroxide nanoparticles to synergize photothermal/photodynamic/chemodynamic cancer therapy. Small Struct 2020;2(2):2000112.
[127] Sun YJ, Feng XR, Wan C, Lovell JF, Jin HL, Ding JX. Role of nanoparticle-mediated immunogenic cell death in cancer immunotherapy. Asian J Pharm Sci 2020;16(2):129–32.
[128] Cheng H, Gadora K, Wang Z, Zhang HQ, Jiang WX, Chen X, et al. Functionalized nanographene oxide in biomedicine applications: bioinspired surface modifications, multidrug shielding, and site-specific trafficking. Drug Discov Today 2019;24(3):749–62.
[129] Lai WF, Wong WT. Use of graphene-based materials as carriers of bioactive agents. Asian J Pharm Sci 2020. doi:10.1016/j.ajps.2020.11.004.
[130] Mitchell MJ, Billingsley MM, Haley RM, Wechsler ME, Peppas NA, Langer R. Engineering precision nanoparticles for drug delivery. Nat Rev Drug Discov 2021;20(2):101–24.
[131] Sun XQ, Liu D, Xu XY, Shen YF, Huang YJ, Zeng ZS, et al. NIR-triggered thermo-responsive biodegradable hydrogel with combination of photothermal and thermodynamic therapy for hypoxic tumor. Asian J Pharm Sci 2020;15(6):713–27.
[132] Zhang HY, Dong SJ, Li ZM, Feng XR, Xu WG, Tulinao CM, et al. Biointerface engineering nanoplatforms for cancer-targeted drug delivery. Asian J Pharm Sci 2020;15(4):397–415.
[133] Choudhary D, Goykar H, Karanwad T, Kannaujia S, Gadekar V, Misra M. An understanding of mitochondria and its role in targeting nanocarriers for diagnosis and treatment of cancer. Asian J Pharm Sci 2020. doi:10.1016/j.ajps.2020.10.002.